AMERICAN SOCIETY FOR MICROBIOLOGY | mBio®

RESEARCH ARTICLE

# Secondary Metabolites Produced during *Aspergillus fumigatus* and *Pseudomonas aeruginosa* Biofilm Formation

**Rafael Wesley Bastos,[a]* Daniel Akiyama,[b] Thaila Fernanda dos Reis,[a] Ana Cristina Colabardini,[a] Rafael Sanchez Luperini,[a] Patrícia Alves de Castro,[a] Regina Lúcia Baldini,[c] Taícia Fill,[b] Gustavo H. Goldman[a]**

[a]Faculdade de Ciências Farmacêuticas de Ribeirão Preto, Universidade de São Paulo, Ribeirão Preto, Brazil
[b]Instituto de Química, Universidade Estadual de Campinas, Campinas, Brazil
[c]Departamento de Bioquímica, Instituto de Química, Universidade de São Paulo, São Paulo, Brazil

**ABSTRACT** In cystic fibrosis (CF), mucus plaques are formed in the patient's lungs, creating a hypoxic condition and a propitious environment for colonization and persistence of many microorganisms. There is clinical evidence showing that *Aspergillus fumigatus* can cocolonize CF patients with *Pseudomonas aeruginosa*, which has been associated with lung function decline. *P. aeruginosa* produces several compounds with inhibitory and antibiofilm effects against *A. fumigatus in vitro*; however, little is known about the fungal compounds produced in counterattack. Here, we annotated fungal and bacterial secondary metabolites (SM) produced in mixed biofilms under normoxia and hypoxia conditions. We detected nine SM produced by *P. aeruginosa*. Phenazines and different analogs of pyoverdin were the main compounds produced by *P. aeruginosa*, and their secretion levels were increased by the fungal presence. The roles of the two operons responsible for phenazine production (*phzA1* and *phzA2*) were also investigated, and mutants lacking one of those operons were able to produce partial sets of phenazines. We detected a total of 20 SM secreted by *A. fumigatus* either in monoculture or in coculture with *P. aeruginosa*. All these compounds were secreted during biofilm formation in either normoxia or hypoxia. However, only eight compounds (demethoxyfumitremorgin C, fumitremorgin, ferrichrome, ferricrocin, triacetylfusigen, gliotoxin, gliotoxin E, and pyripyropene A) were detected during biofilm formation by the coculture of *A. fumigatus* and *P. aeruginosa* under normoxia and hypoxia conditions. Overall, we showed how diverse SM secretion is during *A. fumigatus* and *P. aeruginosa* mixed culture and how this can affect biofilm formation in normoxia and hypoxia.

**IMPORTANCE** The interaction between *Pseudomonas aeruginosa* and *Aspergillus fumigatus* has been well characterized *in vitro*. In this scenario, the bacterium exerts a strong inhibitory effect against the fungus. However, little is known about the metabolites produced by the fungus to counterattack the bacteria. Our work aimed to annotate secondary metabolites (SM) secreted during coculture between *P. aeruginosa* and *A. fumigatus* during biofilm formation in both normoxia and hypoxia. The bacterium produces several different types of phenazines and pyoverdins in response to presence of the fungus. In contrast, we were able to annotate 29 metabolites produced during *A. fumigatus* biofilm formation, but only 8 compounds were detected during biofilm formation by the coculture of *A. fumigatus* and *P. aeruginosa* upon either normoxia or hypoxia. In conclusion, we detected many SM secreted during *A. fumigatus* and *P. aeruginosa* biofilm formation. This analysis provides several opportunities to understand the interactions between these two species.

**KEYWORDS** *Aspergillus fumigatus*, *Pseudomonas aeruginosa*, biofilm formation, gliotoxin, hypoxia and normoxia, secondary metabolites

**Editor** J. Andrew Alspaugh, Duke University Medical Center



Address correspondence to Gustavo H. Goldman, ggoldman@usp.br.

*Present address: Rafael Wesley Bastos, Departamento de Microbiologia e Parasitologia, Universidade Federal do Rio Grande do Norte, Natal, Brazil.

The authors declare no conflict of interest.

**Received** 27 June 2022
**Accepted** 5 July 2022
**Published** 20 July 2022

*Pseudomonas aeruginosa* is a Gram-negative bacterium that grows aerobically and under anaerobic conditions in certain specific circumstances. The species is ubiquitous in nature and has been found inhabiting soil and water and also colonizing humans, where it sometimes acts as an opportunistic pathogen (1). In immunosuppressed, burned, and hospitalized patients, *P. aeruginosa* is responsible for a broad spectrum of serious diseases ranging from acute to chronic infections, such as bloodstream infections in intensive care units, surgical site infections, hospital-acquired pneumonia, respiratory and urinary tract infections, and burn and chronic dermal wound infections (1, 2). *P. aeruginosa* also chronically infects the lungs of people with underlying pulmonary diseases, such as cystic fibrosis (CF).

CF is a genetic disorder caused by mutations in the CF transmembrane conductance regulator gene that result in defective chloride secretion, altered airway surface liquid, ciliary dyskinesis, and impaired mucociliary clearance (3). Such changes lead to motionless mucus plaques, which create a hypoxic condition and a propitious environment for colonization and persistence of many microorganisms, notably *P. aeruginosa* (1, 4). By performing an *in vivo* characterization of CF airways, Worlitzsch and colleagues (4) demonstrated that *P. aeruginosa* forms biofilm-like macrocolonies in the intraluminal site, which is markedly hypoxic due to mucus accumulation. In response to hypoxia, *P. aeruginosa* increases alginate exopolysaccharide production, and that may help the bacteria grow as a biofilm and persist in that environment.

In addition to *P. aeruginosa* and other bacteria, CF lungs can be colonized by fungi, with *Aspergillus fumigatus* the main isolated mold. There is a particular interest in this opportunistic pathogen, as *A. fumigatus* presence in respiratory CF samples has been associated with poorer prognosis and pulmonary function decline (5). *A. fumigatus* is a ubiquitous filamentous fungus encountered in soil, water, air, decomposing organic matter, and plant-based materials (6, 7), and it probably evolved in contact with water and soil bacteria such as *P. aeruginosa*. *A. fumigatus* can cause a range of illnesses that vary from chronic or hypersensitization (allergic reactions) disorders to invasive and life-threatening diseases (8). In CF patients, *A. fumigatus* may colonize the bronchi, which is frequently accompanied by hypersensitization (1, 9, 10), allergic bronchopulmonary aspergillosis (11), and bronchitis (12).

There is clinical evidence that *A. fumigatus* and *P. aeruginosa* cocolonize CF patients, and this is associated with lung function decline. Some reports estimate that 60% of patients with chronic *P. aeruginosa* infection also carry *A. fumigatus* (13–16). Studies investigating how *A. fumigatus* and *P. aeruginosa* affect each other *in vivo* and the outcome of this interaction for the host are limited; however, several studies have analyzed this interaction *in vitro*. Overall, *P. aeruginosa* has a strong inhibitory effect against *A. fumigatus in vitro* (including inhibition of biofilm formation and conidiation), due to bacteria-produced compounds (1, 17). The surfactant dirhamnolipids inhibit fungal growth by blocking $\beta$-1,3-glucan synthase (18), a key enzyme for fungal cell wall production; the quorum-sensing homoserine lactones act to suppress hyphal growth (19); the siderophore pyoverdine causes fungal iron starvation (17, 20, 21); and pyochelin and phenazines kill *A. fumigatus* by inducing oxidative and nitrosative stresses as well as iron starvation (17, 22).

Phenazines are nitrogen-containing colored aromatic molecules which constitute a large group of secondary metabolites (SM) produced by bacteria with broad physiological functions, including acting as antibiotics (2) and antifungals (22–25), involvement in biofilm formation (26), and regulation of gene expression (27). Several phenazines are produced by *P. aeruginosa* (Fig. 1), such as pyocyanin (PYO), phenazine-1-carboxamide (PCN), phenazine-1-carboxylic acid (PCA), 1-hydroxyphenazine (1-HP), and 5-methyl-phenazine-1-carboxylic acid (5-Me-PCA). Biosynthesis of PCA from chorismic acid requires enzymes coded by two sets of homologous genes (*phzABCDEFG*) located in two nearly identical redundant operons (*phz1* and *phz2*) that have different promoters and flanking regions (28). Another three genes, *phzM*, *phzS*, and *phzH*, code for enzymes that convert PCA to PYO and PCN and are located next to either *phz1* or *phz2* operons (28).

Although *P. aeruginosa* compounds with inhibitory and antibiofilm effects against *A. fumigatus* have been revealed, little is known about the compounds produced by the fungus during the interaction. Furthermore, most of the studies about *P. aeruginosa* SM during

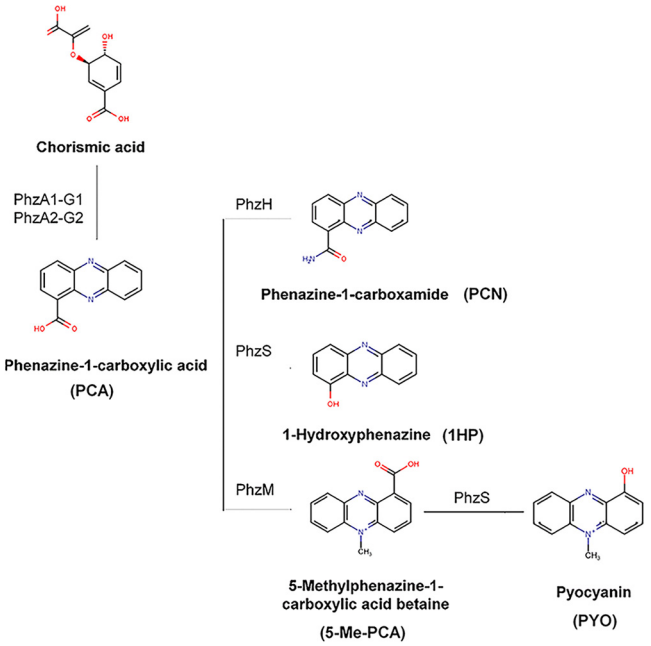


**FIG 1** *P. aeruginosa* phenazine biosynthesis pathway.

interactions were done by using mutants lacking important genes for biosynthesis of such compounds and/or by measuring the effect of adding purified compounds or bacteria-filtered supernatant to the coculture or a monoculture. There is a lack of studies identifying fungal and bacterial SM produced throughout coculturing and mixed biofilms and their roles in the fungus-bacterium interaction, especially regarding fungal metabolites.

Here, we show the SM produced by *P. aeruginosa* and *A. fumigatus* in single or mixed biofilms during normoxia and hypoxia conditions. We detected 10 SMs produced by *P. aeruginosa*. Phenazines and different analogs of pyoverdin were the main compounds produced by *P. aeruginosa*, and their secretion levels were increased by the fungal presence. The contributions of the two operons that regulate phenazine production (*phzA1* and *phzA2*) are still controversial and were also investigated. The results showed that Δ*phzA1* and Δ*phzA2* mutants can produce a subset of phenazines when in hypoxia and in the presence of the fungus. In contrast, we were able to detect 20 SM produced by *A. fumigatus*, but only 8 of them (demethoxyfumitremorgin C, fumitremorgin C, ferrichrome, ferricrocin, triacetylfusigen, gliotoxin, gliotoxin E, and pyripyropene A) were produced in the presence of *P. aeruginosa*.

## RESULTS

***A. fumigatus* and *P. aeruginosa* biofilm formation in normoxia and hypoxia.** We established a protocol for *P. aeruginosa* and *A. fumigatus* biofilm formation under normoxia and hypoxia by using $10^5$ CFU/mL from exponential-phase *P. aeruginosa* cultures and $10^6$ *A. fumigatus* conidia/mL (Fig. 1). *P. aeruginosa* wild type and Δ*phzA1* (A1) and Δ*phzA2* (A2) mutant strains were comparable in biofilm formation. Mixed biofilms of *A. fumigatus-P. aeruginosa*, *A. fumigatus-P. aeruginosa* Δ*phzA1* (AfA1), and AfA2 had more biomass than bacteria-only biofilms, in either normoxia or hypoxia (Fig. 2A and B). However, *A. fumigatus* biofilms without bacteria produced more biomass than mixed biofilms, indicating an antagonistic role of *P. aeruginosa* toward *A. fumigatus* biofilm formation.

These results were refined by estimating the *P. aeruginosa* and *A. fumigatus* DNA copy number by quantitative PCR (qPCR) using *P. aeruginosa ecfX* (encoding an extracytoplasmic function sigma factor unique to *P. aeruginosa*, also annotated as *hxuI*) and *gyrB* (encoding a DNA gyrase) and *A. fumigatus* 18S DNA (29–31). Corroborating the biofilm biomass results, *A. fumigatus* DNA copy number decreased in the presence of any *P. aeruginosa* strain under all conditions (Fig. 2C and D). Under normoxia conditions, we observed that *P. aeruginosa* wild type and A1 DNA copy number increased in the presence of *A. fumigatus*, but this was

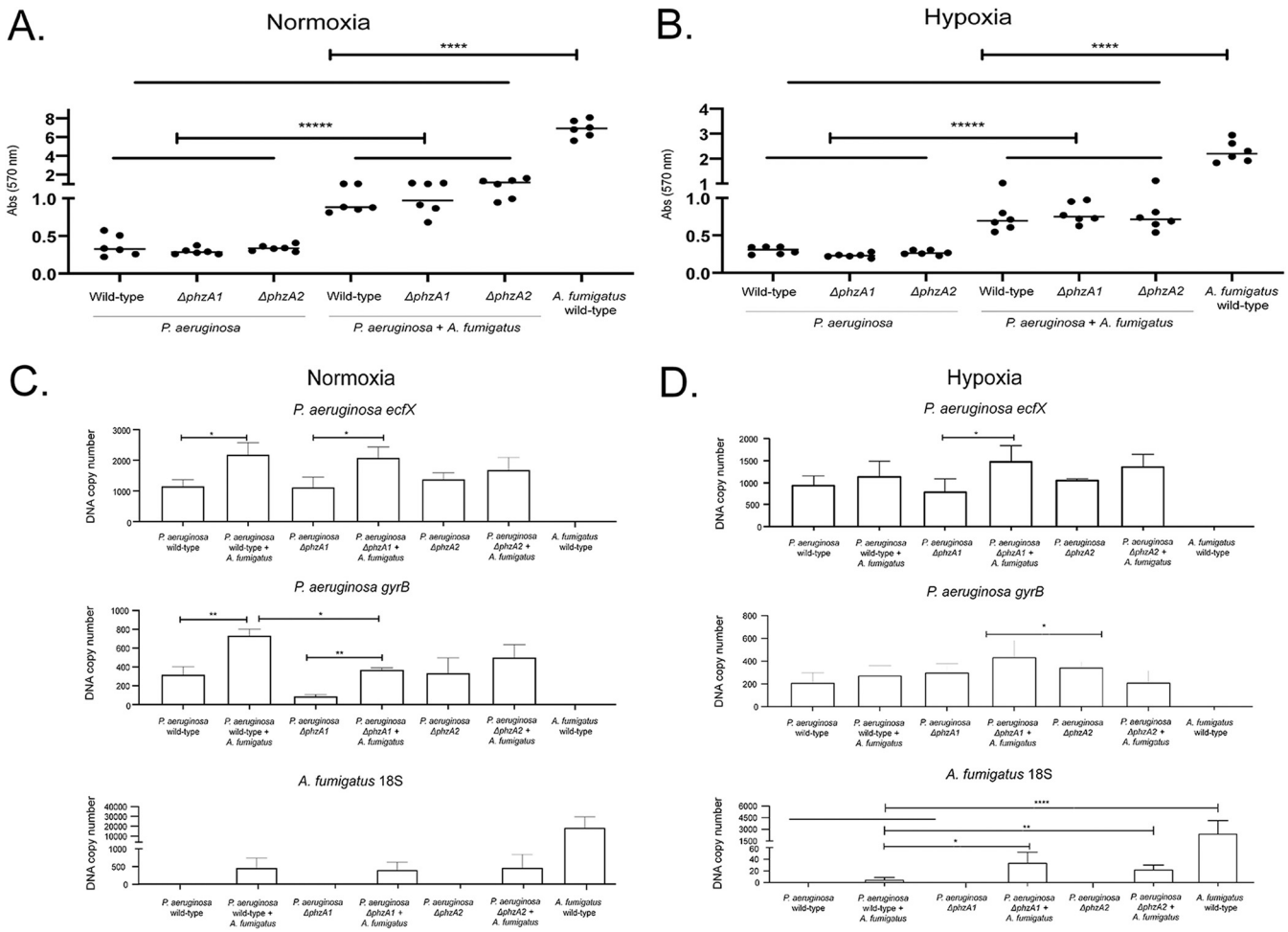


**FIG 2** Biofilm formation by *P. aeruginosa* and *A. fumigatus*. (A and B) *P. aeruginosa* and *A. fumigatus* grown for 5 days at 37°C in normoxia and hypoxia conditions. The results of the absorbance of crystal violet are the average of six repetitions ± standard deviations. (C and D) qPCR results for *P. aeruginosa efcX* and *gyrB* and *A. fumigatus* 18S DNA. The results are the averages of three repetitions ± standard deviations. *, $P < 0.05$; **, $P < 0.01$; ****, $P < 0.0001$; *****, $P < 0.00001$.

not true for A2, which showed the same DNA copy number with or without *A. fumigatus* (Fig. 2C). In contrast, under hypoxia conditions, only AfA1 showed a higher *P. aeruginosa* DNA copy number than A1 alone (Fig. 2D); interestingly, increased *A. fumigatus* DNA copy number was observed in AfA1 and AfA2 cultures compared to the *A. fumigatus-P. aeruginosa* wild type (Fig. 2D). This suggests that *P. aeruginosa phz* mutant strains have a lower ability to inhibit *A. fumigatus* biofilm than the *P. aeruginosa* wild-type strain.

These results strongly indicate that we have established a robust *A. fumigatus-P. aeruginosa* biofilm formation protocol under normoxia and hypoxia conditions.

**Secondary metabolites produced by *P. aeruginosa* during biofilm formation.** Next, we used high-performance liquid chromatography (HPLC)–high-resolution tandem mass spectrometry ($HRMS^2$) to identify SM in the *A. fumigatus* and *P. aeruginosa* biofilm supernatants. We were able to annotate a total of 29 SM, 9 from *P. aeruginosa* and 20 from *A. fumigatus*, in the supernatants produced under either condition (Fig. 3; see also our supplementary data available via figshare, including Table S1 and Fig. S1 to S8, at https://doi.org/10.6084/m9.figshare.19620702). PhZA1-G1 and PhZA2-G2 pathways use chorismic acid as the precursor for transformation into PCA (Fig. 1). PCA is converted into phenazine-1-carboxamide, 1-hydroxyphenazine, and 5-methylphenazine-1-carboxylic acid betaine by PhzH, PhzS, and PhzM, respectively (Fig. 1). Subsequently, 5-methylphenazine-1-carboxylic acid betaine is converted into pyocyanin by PhzS (Fig. 1). As expected, methylphenazine-1-carboxylic acid betaine and pyocyanin were not detected in the Δ*phzA1* mutant (A1 biofilm) under normoxia conditions (Fig. 3 and Fig. 4C and E). All these compounds, except for methylphenazine-1-carboxylic acid betaine, were induced in the mixed *A. fumigatus-P. aeruginosa* biofilm under

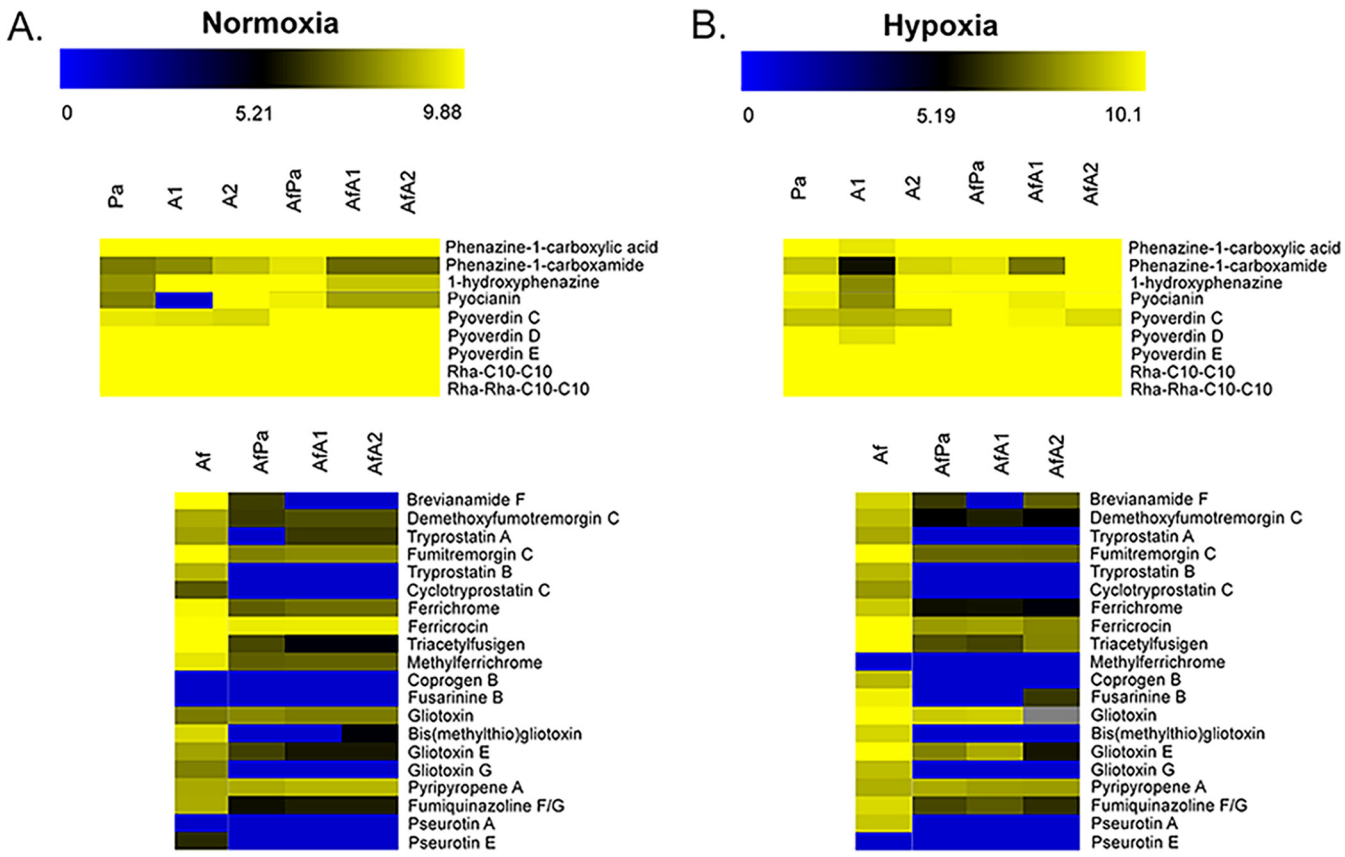


**FIG 3** Specialized secondary metabolite production by *P. aeruginosa* and *A. fumigatus*. Heat maps depict the $\log_{10}$ of the area of chromatograms of 29 SM (9 from *P. aeruginosa* and 20 from *A. fumigatus*). The values represent the averages of three independent biological repetitions. Pa, *P. aeruginosa*; Af, *A. fumigatus*.

normoxia and hypoxia conditions, compared to a *P. aeruginosa*-only biofilm (Fig. 3 and Fig. 4A to E). Interestingly, the production of phenazines in A1 and A2 biofilms varied compared to those in the wild-type *P. aeruginosa* biofilm: whereas A1 presented low phenazine production under all conditions, A2 had higher phenazine production than wild-type *P. aeruginosa* or A1.

When phenazine production by AfA1 mixed biofilms was analyzed, there was an increase for all compounds under both normoxia and hypoxia conditions, compared to the A1-only biofilm; however, AfA2 biofilms only increased phenazine production under hypoxia, compared to A2-only biofilms, except for PYO. Phenazine-1-carboxamide production was comparable in the *P. aeruginosa* wild-type and A1 strains under hypoxia conditions (Fig. 3 and Fig. 4A to E). Phenazine production in AfA1 was much lower than that of *A. fumigatus-P. aeruginosa* wild type under either condition (Fig. 3 and Fig. 4A to E). As expected, phenazine production was significantly higher during biofilm formation in hypoxia than normoxia (Fig. 3 and Fig. 4A to F), as PYO can be used as an alternative electron acceptor in anaerobiosis (32).

The siderophores pyoverdine C, D, and E and rhamnolipids Rha-$C_{10}$-$C_{10}$ and Rha-Rha-$C_{10}$-$C_{10}$ are produced in comparable amounts during biofilm formation by *A. fumigatus-P. aeruginosa* wild type, A1, and A2 under normoxia and hypoxia conditions (Fig. 3 and Fig. 5). The Δ*phzA1* and Δ*phzA2* mutations affected pyoverdin D and E levels during biofilm formation in hypoxia (Fig. 3 and Fig. 5B and C). All these compounds were produced in larger amounts in mixed biofilms (*A. fumigatus-P. aeruginosa* wild type, AfA1, and AfA2) in both normoxia and hypoxia, except for pyoverdine E under normoxia (Fig. 3 and Fig. 5A to E).

These results indicated that interaction with *A. fumigatus* in mixed biofilms stimulates the production of phenazines by the *P. aeruginosa* wild-type strain and that mutation in *phzA1* or *phzA2* modulates negatively or positively phenazine production, respectively. Pyoverdine and rhamnolipid production are not significantly different among *P. aeruginosa* wild type, A1, and

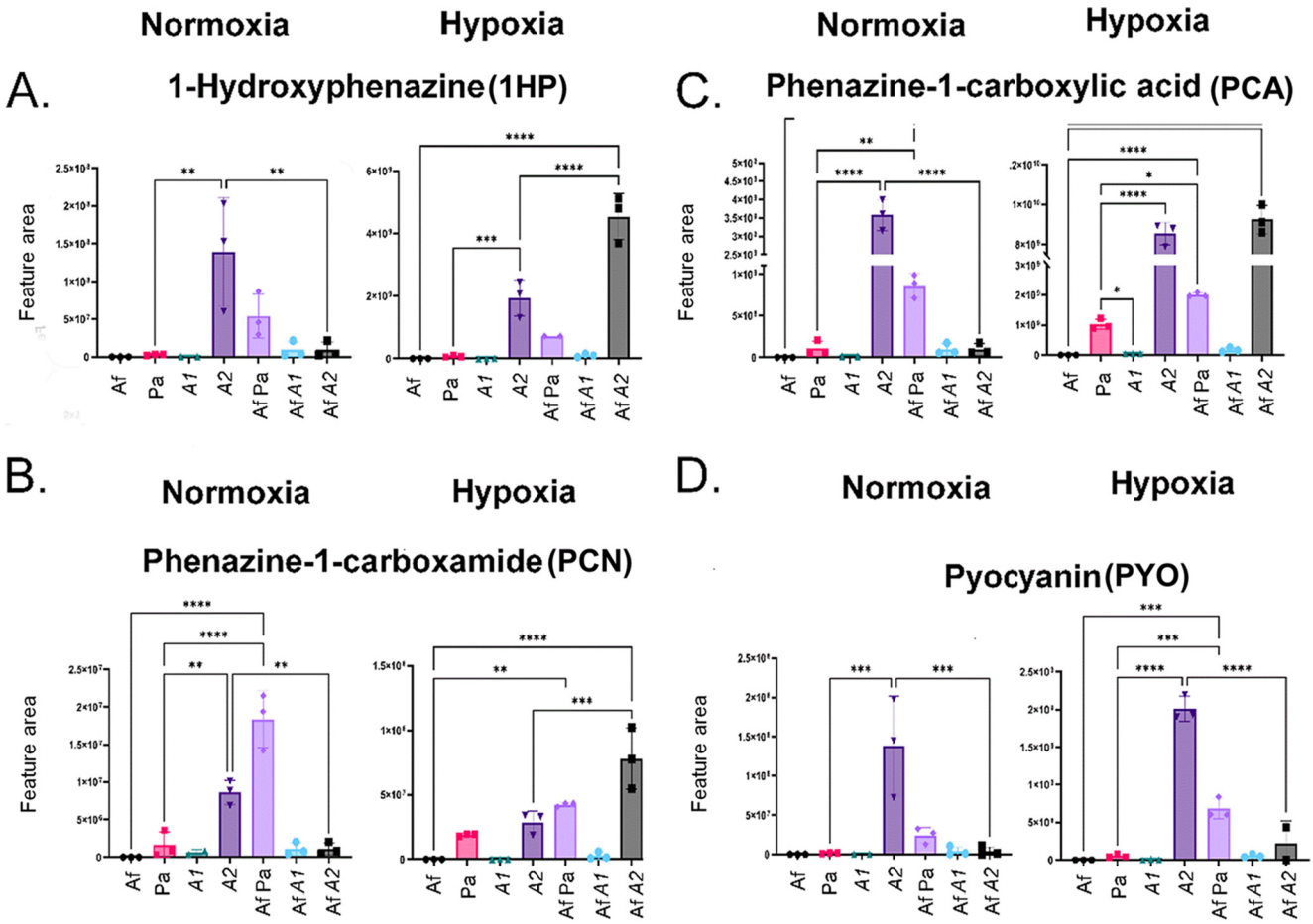


**FIG 4** *P. aeruginosa* phenazine production during biofilm formation in normoxia and hypoxia. Areas of the chromatograms of 1-hydroxyphenazine (A), phenazine-1-carboxylic acid (B), phenazine-1-carboxamide (C), and pyocyanin (D) are shown. The results are the averages of three repetitions ± standard deviations. *, $P < 0.05$; **, $P < 0.01$; ***, $P < 0.001$; ****, $P < 0.0001$.

A2, but increased production was detected in all mixed biofilms (*A. fumigatus-P. aeruginosa* wild type, AfA1, and AfA2).

***A. fumigatus* biofilm formation induces the production of metabolites in the superpathway of fumitremorgin biosynthesis.** The tremorgenic mycotoxins in the group fumitremorgins are prenylated indole alkaloids produced by *A. fumigatus* (33). Fumitremorgin C is produced through a series of steps in the superpathway of fumitremorgin biosynthesis (http://vm-trypanocyc.toulouse.inra.fr/META/NEW-IMAGE?type=PATHWAY&object=PWY-7525&orgids=LEISH) (Fig. 6A). Several metabolites in this pathway are produced during biofilm formation under normoxia and hypoxia conditions, such as brevianamide F, demethoxyfumitremorgin C, tryprostatin A, fumitremorgin C, tryprostatin B, and cyclotryprostatin (Fig. 3 and Fig. 6B to G). Although with lower production than those produced by *A. fumigatus*, the *A. fumigatus-P. aeruginosa* biofilm showed production of brevianamide F (in hypoxia), demethoxyfumitremorgin C (in normoxia and hypoxia), and fumitremorgin C (in normoxia and hypoxia); there were no differences between *A. fumigatus-P. aeruginosa* wild type, AfA1, and Af2 (Fig. 3 and Fig. 6B, E, and F). These results indicated that *A. fumigatus* is able to produce several metabolites in the superpathway of fumitremorgin biosynthesis during biofilm formation and in the presence of *P. aeruginosa*.

**There is increased production of *A. fumigatus* metabolites important for iron metabolism during biofilm formation.** We annotated several metabolites relevant for iron assimilation, such as ferrichrome, ferricrocin, and triacetylfusigen, produced during *A. fumigatus* biofilm formation under normoxia and hypoxia conditions (Fig. 3 and Fig. 7A to C). Methyl ferrichrome was produced by *A. fumigatus* in biofilms only under normoxia (Fig. 3 and Fig. 7D), while

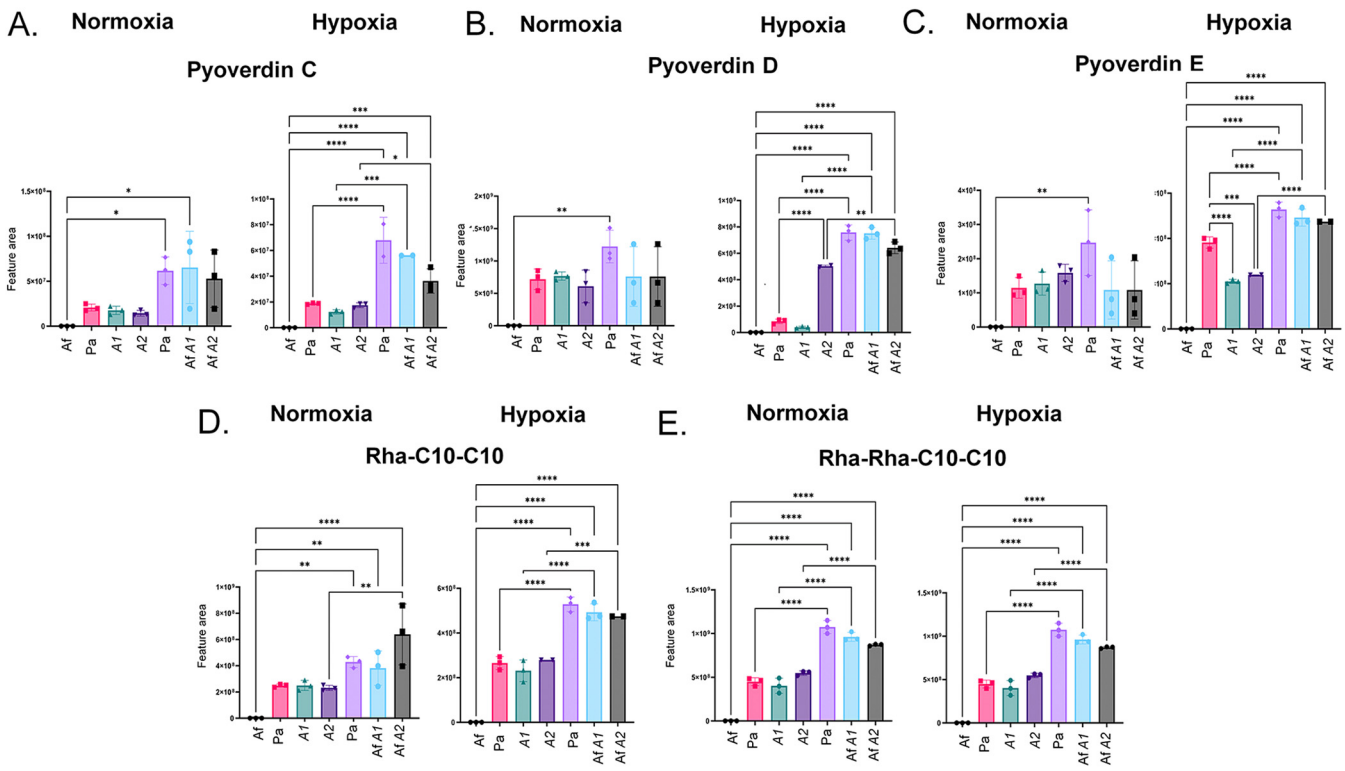


**FIG 5** *P. aeruginosa* pyoverdin and rhamnolipid production during biofilm formation in normoxia and hypoxia. Areas of the chromatograms of pyoverdin C (A), pyoverdin D (B), pyoverdin E (C), Rha-$C_{10}$-$C_{10}$ (D), and Rha-Rha-$C_{10}$-$C_{10}$ (E) are shown. The results are the averages of three repetitions ± standard deviations. *, $P < 0.05$; **, $P < 0.01$; ***, $P < 0.001$; ****, $P < 0.0001$.

coprogen B and fusarinine B were produced only under hypoxia conditions (Fig. 3 and Fig. 7E and F). Ferrichrome, ferricrocin, and triacetylfusigen were produced during biofilm formation by the mixed fungus-bacteria culture under both normoxia and hypoxia conditions, although at levels 10- to 1,000-fold lower than in *A. fumigatus*-only biofilms (Fig. 3 and Fig. 7A, B, and C). *P. aeruginosa* wild type and the mutant strains (A1 and A2) behaved in similar patterns regarding the production of those compounds, with a few exceptions: AfA1 biofilms did not produce ferrichrome in hypoxia or triacetylfusigen in normoxia.

Taken together, these results strongly indicate that *A. fumigatus* can still produce several metabolites important for iron chelation during biofilm formation in both normoxia and hypoxia conditions, notably, ferrichrome, ferricrocin, and triacetylfusigen. Nevertheless, the results also showed that *P. aeruginosa* strongly affects the overall production of all iron chelators detected in this approach, suggesting that competition for this micronutrient is a key point in the *A. fumigatus*-*P. aeruginosa* interaction in biofilms.

**Gliotoxin, pyripyropene A, and fumiquinazoline F and G are produced by *A. fumigatus* during biofilm formation.** Gliotoxin (GT) and GT-modified forms, such as bis(methylthio) GT, GT E, and GT G, are produced during *A. fumigatus* biofilm formation under normoxia and hypoxia conditions (Fig. 3 and Fig. 8A to D). GT production was induced 2- to 3-fold induced in the *A. fumigatus*-*P. aeruginosa* wild type, AfA1, and AfA2 cultures during biofilm formation under normoxia conditions (Fig. 3 and Fig. 8A). Curiously, under hypoxia conditions, GT levels were lower than the *A. fumigatus*-only culture in the mixed biofilms, and the lack of *phzA2* function suppressed GT production completely (Fig. 3 and Fig. 8B). Pyripyropene A was produced in comparable levels in all conditions, both in *A. fumigatus*-only and mixed biofilms (Fig. 3 and Fig. 8E), indicating that the presence of *P. aeruginosa* did not influence its production. A different pattern was seen for the production of fumiquinazoline F or G in mixed biofilms, as production was completely inhibited by the bacteria in normoxia but only partially during hypoxia (Fig. 3 and Fig. 8F).

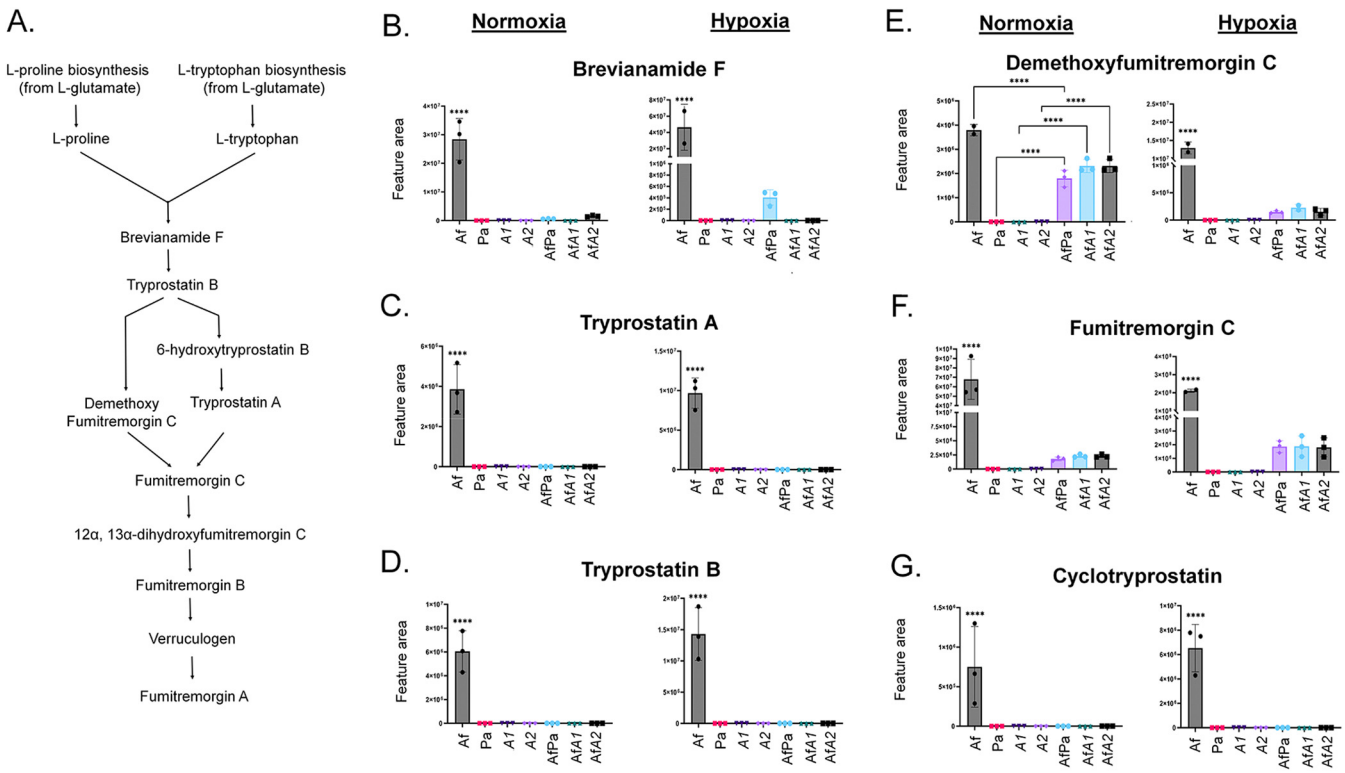


**FIG 6** *A. fumigatus* biofilm formation induces the production of metabolites in the superpathway of fumitremorgin biosynthesis. (A) Superpathway of fumitremorgin biosynthesis. (B to G) Areas of the chromatograms of brevianamide F (B), tryprostatin A (C), tryprostatin B (D), demethoxyfumitremorgin C (E), fumitremorgin C (F), and cyclotryprostatin (G). The results are the averages of three repetitions ± standard deviations. ****, $P < 0.0001$.

Taken together, these results emphasize the importance of GT, pyripyropene A, and fumiquinazoline F and G during *A. fumigatus-P. aeruginosa* biofilm formation and suggest that *A. fumigatus* uses GT as a defense against *P. aeruginosa*.

**Biofilm formation in the presence of *A. fumigatus* mutants impaired in SM production.** As a preliminary step to investigate if *A. fumigatus* SM are important for the establishment of *A. fumigatus-P. aeruginosa* biofilm formation under normoxia and hypoxia conditions, we tested several mutants impaired in the production of (i) gliotoxin (Δ*gliT*; *gliT* encodes an oxidoreductase), (ii) pseurotin (Δ*psoF*; *psoF* encodes a putative enzyme with dual function as a methyltransferase and monooxygenase), (iii) fumiquinazoline (Δ*fmqA*; *fmqA* encodes a nonribosomal peptide synthetase), and (iv) fumagillin and pseurotin (Δ*fapR*; *fapR* encodes a transcription factor) (Fig. 9). All these mutants, except for Δ*fmqA*, had radial growth on RPMI medium comparable to that of the wild-type strain in both normoxia and hypoxia conditions (Fig. 9A).

qPCR analysis showed that *A. fumigatus* Δ*psoF* and Δ*fmqA* had increased biofilm formation during normoxia in the absence and presence of *P. aeruginosa* (Fig. 9B). However, Δ*gliT* had decreased biofilm formation during normoxia only in the presence of *P. aeruginosa* (Fig. 9B). There were fewer *P. aeruginosa* cells in the biofilm dual interaction between *A. fumigatus* Δ*psoF* or Δ*fapR* and *P. aeruginosa* during normoxia conditions (Fig. 9C), while there were no statistically significant differences in the number of *P. aeruginosa* cells in the presence of other *A. fumigatus* mutants (Fig. 9C). No differences were observed between the *A. fumigatus* 18S wild type and mutants or with *P. aeruginosa ecfX* with *A. fumigatus* wild type and mutants during biofilm formation under hypoxia conditions (Fig. 9D and E).

These results suggest that gliotoxin is important for *A. fumigatus-P. aeruginosa* biofilm formation during normoxia conditions. Curiously, the lack of pseurotin production decreased *P. aeruginosa* biofilm formation during normoxia conditions, while the secondary metabolite mutants did not affect *A. fumigatus-P. aeruginosa* biofilm formation during hypoxia conditions.

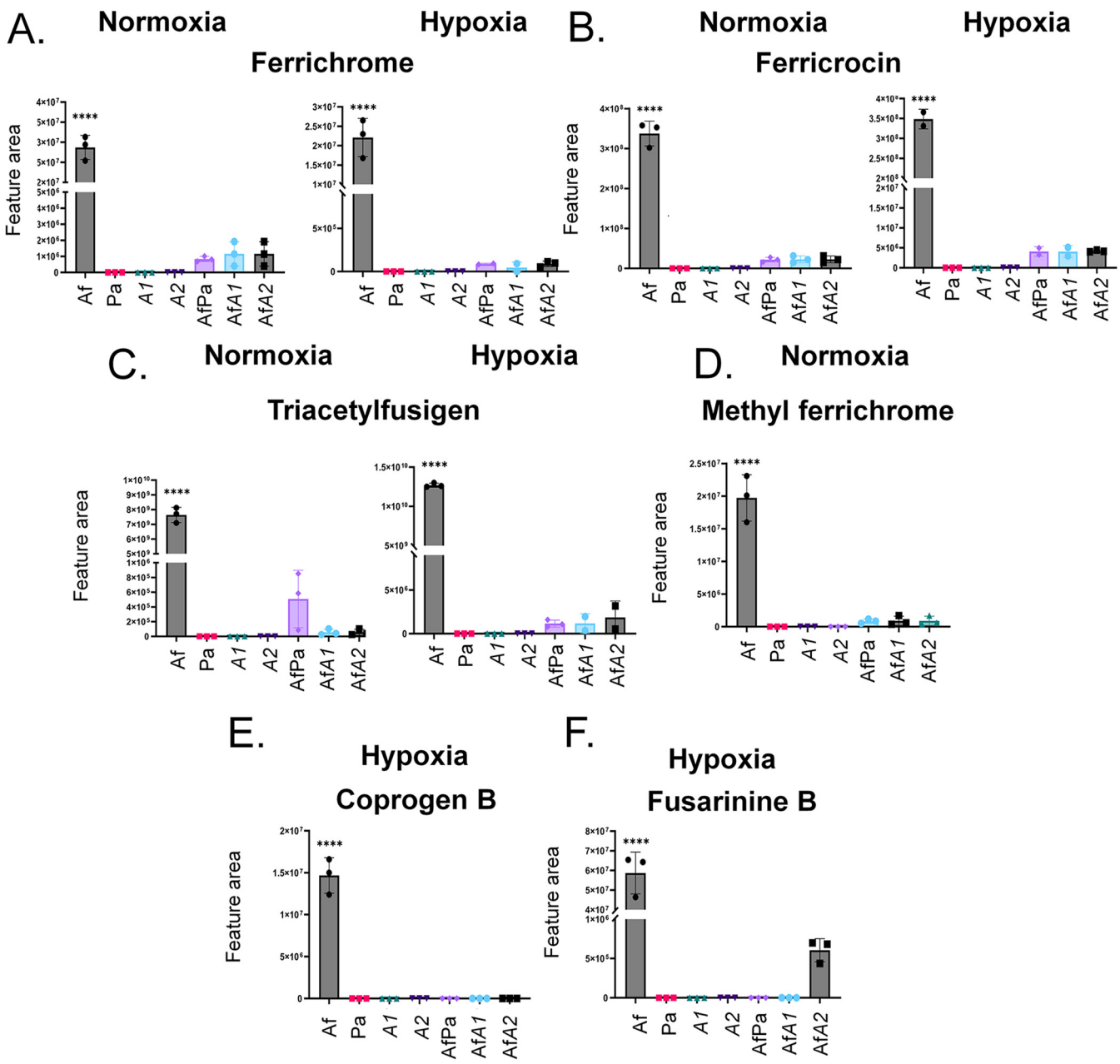


**FIG 7** There is increased production of *A. fumigatus* metabolites important for iron metabolism during biofilm formation. Areas of the chromatograms of ferrichrome (A), ferrichrocin (B), triacetylfusigen (C), methylferrichrome (D), coprogen B (E), and fusarinine B (F) are shown. The results are the averages of three repetitions ± standard deviations. ****, $P < 0.0001$.

## DISCUSSION

The clinical and scientific interests in coinfection with *A. fumigatus* and *P. aeruginosa* are due to its association with a decline in the lung function in cystic fibrosis patients, which has been shown in many reports (1). Inside the host, both pathogens have to face a hostile environment triggering general and specific responses and adapting to specific conditions and nutrient availability. Furthermore, they may interact with each other, which can boost their growth or lead to the production of antagonistic molecules. Among such molecules, some SM have been described as affecting fungal and bacterial growth and their metabolism. However, to the best of our knowledge, an overview of SM production by both microorganisms in cocultivation is missing. It is important that we have not worked with *A. fumigatus* and *P. aeruginosa* clinical isolates that chronically colonize patient lungs. *A. fumigatus* CEA17 is a derivative of CEA10, a clinically derived strain isolated from a patient with invasive aspergillosis (34–36). *P.*

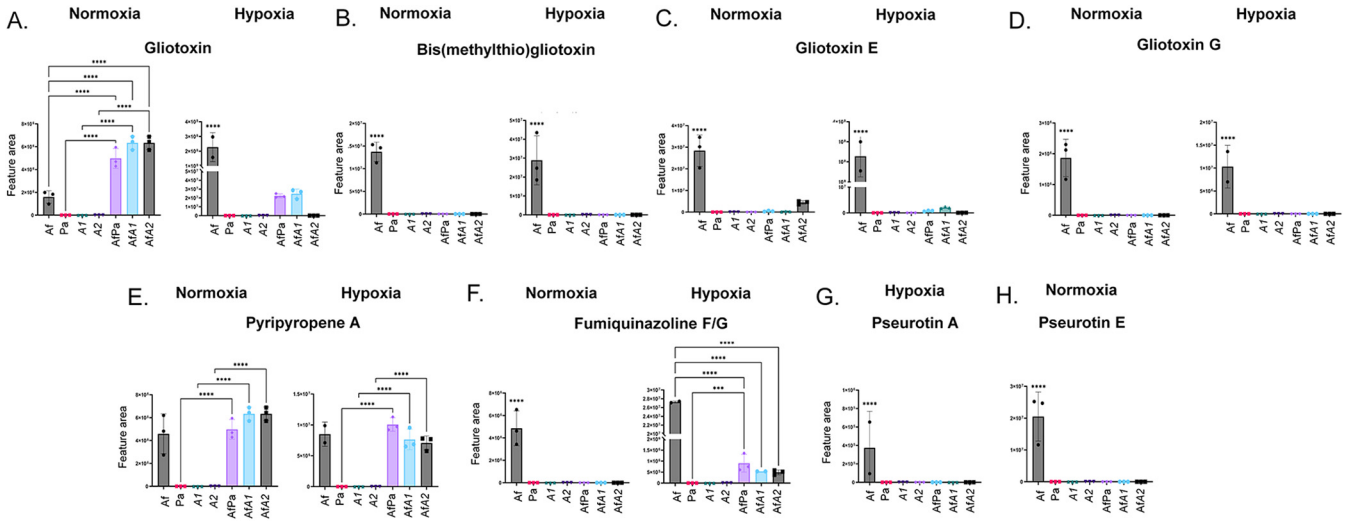


**FIG 8** Gliotoxin, pyripyropene A, and fumiquinazoline F and G are produced during *A. fumigatus* biofilm formation. Areas of the chromatograms of gliotoxin (A), bisdethiobis(methylthio)-gliotoxin (B), gliotoxin E (C), gliotoxin G (D), pyripiropene A (E), fumiquinazoline F and G (F), pseurotin A (G), and pseurotin E (H) are shown. The results are the averages of three repetitions ± standard deviations. ***, $P < 0.001$; ****, $P < 0.0001$.

*aeruginosa* PA14, a highly virulent isolate that represents the most common clonal group worldwide, was isolated from a burn wound and not from a patient lung (37). However, we decided to work with these two clinical isolates because they have several technological resources, for instance, deletion and disruption libraries of their whole genomes, that will favor further investigation of the biological basis of their interaction. It is possible that clinical isolates of both species that are colonizing the lungs of CF patients have different SM profiles from what is described here, and this remains to be investigated. Another important observation is that the reduced production of an *A. fumigatus* SM does not reflect the direct inhibition of its biosynthesis by *P. aeruginosa*. This could be due to the effect of *A. fumigatus* growth inhibition by *P. aeruginosa*, since less fungal biomass in the mixed biofilms likely produces less metabolites.

Here, we showed that *P. aeruginosa* has antagonistic effects against *A. fumigatus* in mixed biofilms, both in normoxic and hypoxic conditions, which is in agreement with reports showing antagonistic action for bacteria isolated from clinical pulmonary samples in a normal oxygen atmosphere (23, 38) and another report that showed that *P. aeruginosa* inhibitory effects were effective independently of the local oxygen pressure (39). *P. aeruginosa* is a nonfermentative bacterium that grows anaerobically when nitrate is available, which may also be a key factor for cultivation in hypoxic conditions (39). In our work, we decided to use RPMI 1640 buffered with HEPES (pH 7.0) because it is a medium that has been used to induce biofilm formation and mimics the human plasma constitution. RPMI 1640 has calcium nitrate [$Ca(NO_3)_2$; 0.42 mM], which could support *P. aeruginosa* growth in hypoxia. *P. aeruginosa* can also survive in oxygen-limited conditions using pyocyanin as an electron acceptor to regenerate $NAD^+$ (40). We performed species-specific qPCR to distinguish between *A. fumigatus* and *P. aeruginosa* in cocultured biofilms and found that *A. fumigatus* growth was inhibited by the presence of *P. aeruginosa* wild type and Δ*phzA1* and Δ*phzA2* mutants independently of the oxygen pressure. However, *P. aeruginosa* wild type and Δ*phzA1* showed increased growth when cocultured with *A. fumigatus* in normoxia. This result disagrees with the work performed by others (41) that showed a mutually antagonistic relationship between *P. aeruginosa* and *A. fumigatus*, but it confirms the data of Margalit and colleagues (42), who demonstrated that the *A. fumigatus* secretome could stimulate the growth of *P. aeruginosa*. Specifically, *A. fumigatus* can produce an amino acid-rich environment in which *P. aeruginosa* can proliferate better in cocultures (42). The increased *P. aeruginosa* proliferation was not observed under hypoxic conditions. We hypothesize that this occurred because the fungus does not grow well in hypoxia and possibly did not create this amino acid-rich environment that is able to boost *P. aeruginosa* growth. Moreover, the *P. aeruginosa* growth rate

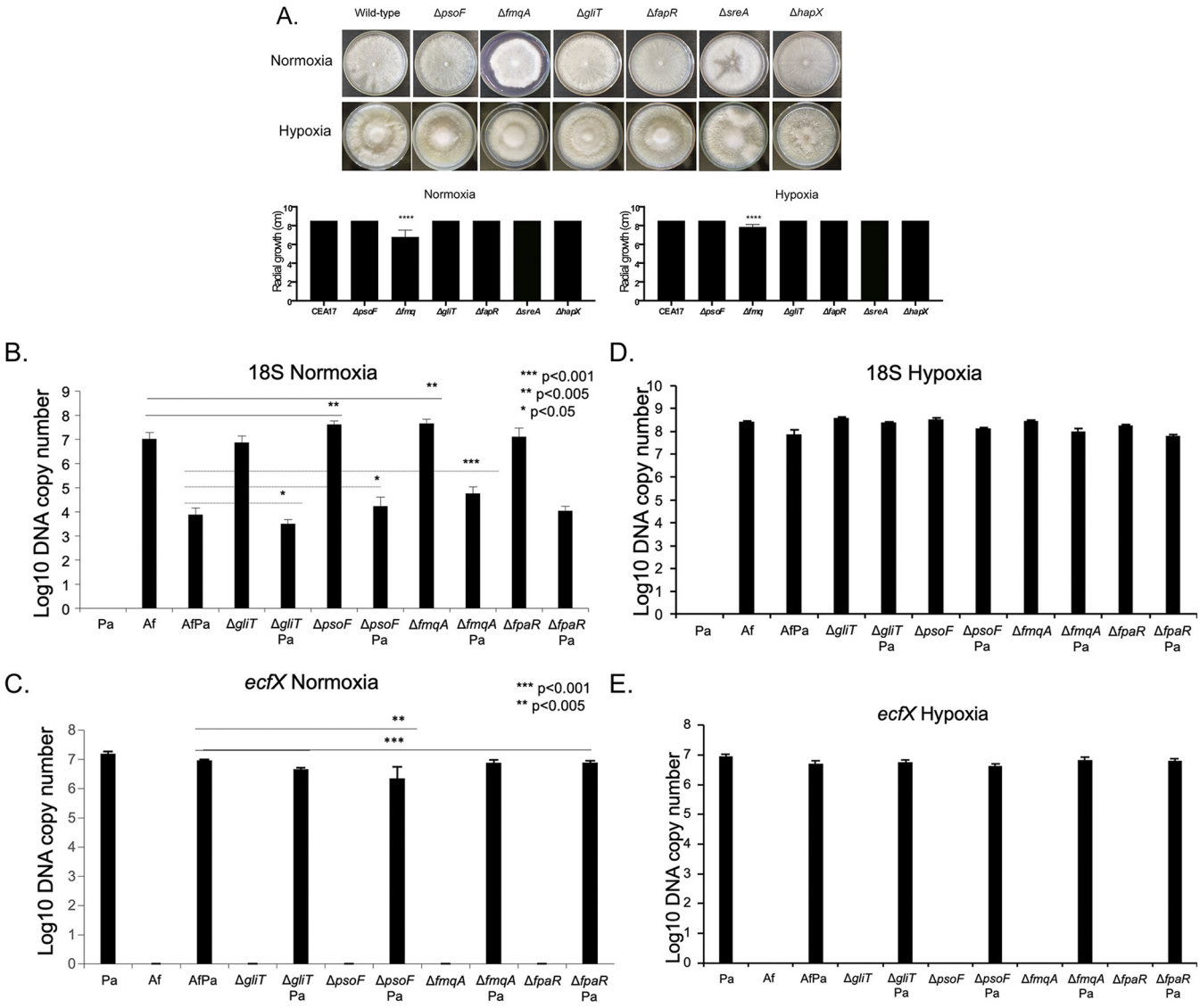


**FIG 9** Gliotoxin is important for *A. fumigatus-P. aeruginosa* biofilm formation. (A) The wild-type and mutant strains were grown for 5 days at 37°C in normoxia and hypoxia conditions. ****, $P < 0.0001$. (B and C) qPCR for *A. fumigatus* 18S DNA (B) and *P. aeruginosa ecfX* (C) biofilm formation under normoxia conditions. (D and E) qPCR for *A. fumigatus* 18S DNA (D) and *P. aeruginosa ecfX* (E) biofilm formation under hypoxia conditions.

in hypoxia is lower than in aerobic conditions, even in the presence of nitrate and arginine, which can also be used as terminal electron acceptors (43).

The antifungal effect of *P. aeruginosa*-produced compounds on *A. fumigatus* has been extensively studied, and several molecules can interfere with fungal morphology, physiology, and growth. In our work, we annotated many phenazines, such as PYO, PCN, PCA, and 1-HP, that are produced by the bacterium in single and mixed cultures, both in hypoxia and normoxia. The antagonistic actions of phenazines are attributed to their redox potential, since reduced phenazines are oxidized in the fungal cell by oxygen and NADPH through a NapA-dependent oxidative stress response, generating reactive oxygen species (ROS) (17, 22). All phenazines at high concentrations induce ROS and reactive nitrogen species (RNS) production by *A. fumigatus* mitochondria, which are released into the cytoplasm and lead to fungal death (44). 1-HP is the most active phenazine against *A. fumigatus* and, in addition to ROS and RNS production, its high inhibitory activity is due to a specific iron chelation property (45). *P. aeruginosa* phenazine production is controlled by a complex regulatory network that involves quorum sensing and catabolite repression (44). Two redundant *phz* gene operons are responsible for phenazine-1-carboxylate production (46–49). Earlier work showed that in *P. aeruginosa* colony biofilms, *phzA2* was expressed at high levels whereas *phzA1* was the most

important operon for PCA production (47). Recent analysis suggested a dominant role of *phzA2*, resulting in a 10-fold-higher expression of *phzA2* compared to *phzA1*, and *phzA2* operon as the main responsible for PCA production (49), but there are marked differences in quorum-sensing regulated traits depending on the particular *P. aeruginosa* strain and specific growth conditions. Surprisingly, in contrast, our results showed that PC production is higher with the Δ*phzA2* strain both in monoculture or *A. fumigatus* coculture than in the Δ*phzA1* mutant.

Another *P. aeruginosa*-produced compound that is induced upon iron starvation is pyoverdine (17), and some authors have shown that this is the main mediator of antifungal activity on *A. fumigatus* biofilms (17, 20). Also, there have been some reports describing that pyoverdine is produced in lower levels under iron-limiting conditions (20) or under hypoxia (39). However, our results showed that *P. aeruginosa* is able to produce pyoverdine in RPMI medium, which is a poor-iron medium, and in a low-oxygen atmosphere. Except for pyoverdine D, there is little influence of the Δ*phzA1* and Δ*phzA2* null mutations on the production of pyoverdine C, D, or E, as expected, since the regulation of phenazines and pyoverdine are independent.

Under our conditions, the rhamnolipids Rha-$C_{10}$-$C_{10}$ and Rha-Rha-$C_{10}$-$C_{10}$ were also detected in all *P. aeruginosa* strain supernatants, and growth in coculture with *A. fumigatus* increased their concentration (Fig. 4D and E). Rhamnolipids are surfactants released by *P. aeruginosa* that have several roles, such as allowing swarming motility and solubilizing hydrophobic compounds that can be used as carbon and energy sources. In host-pathogen interactions, rhamnolipids are considered virulence factors, as they may help to lyse host cell membranes, interfere with signaling pathways, and solubilize the lung surfactant. They are also toxic to other bacteria, fungi, and other microorganisms, conferring a competitive advantage in colonizing multiple environments (50). In mixed *A. fumigatus-P. aeruginosa* biofilms, the induction of rhamnolipid production might be one of the factors that interferes with *A. fumigatus* growth, but the specific role of rhamnolipids in these interactions could not be addressed in this work.

Recently, quantitative proteomic analysis showed that *A. fumigatus* exposed to *P. aeruginosa* culture filtrate had increased expression of proteins involved in SM biosynthesis, such as gliotoxin, fumagillin, and pseurotin A (51). To shed light on how *A. fumigatus* responds to all these compounds produced by *P. aeruginosa*, we also annotated and performed relative quantification of fungal SM. We detected 20 SM secreted by *A. fumigatus* either in monoculture or in coculture with *P. aeruginosa*. All these compounds were secreted during fungal biofilm formation either in normoxia or hypoxia. However, we were only able to detect and annotate eight compounds (demethoxyfumitremorgin C, fumitremorgin, ferrichrome, ferricrocin, triacetylfusigen, gliotoxin, gliotoxin E, and pyripyropene A) produced during biofilm formation by the coculture of *A. fumigatus* and *P. aeruginosa* upon either normoxia or hypoxia conditions. Interestingly, brevianamide F and fumiquinazoline F and G were produced only upon hypoxia conditions, while methyl ferrichrome was produced only upon normoxia conditions. These results indicate that these SM are important for the interaction between *A. fumigatus* and *P. aeruginosa*, and the production of some of them is regulated by the oxygen condition. Of note, gliotoxin was the only SM produced in higher levels in mixed biofilms compared to *A. fumigatus*-only biofilms, suggesting that the fungus specifically overproduces this compound in response to the bacterial antagonist. Gliotoxin has been the most well-studied and characterized SM from *A. fumigatus*, and it is also important for the interaction with *P. aeruginosa* and for biofilm formation (52, 53). Reece and colleagues (41) showed that gliotoxin has an antibacterial activity and antibiofilm effect against several bacteria, including *P. aeruginosa*. Our results emphasize the importance of gliotoxin during the interaction between *A. fumigatus* and *P. aeruginosa*, because it is the only compound produced by *A. fumigatus* in significantly higher amounts in mixed biofilms than by *A. fumigatus*-only biofilms, despite the lower fungal DNA copy number in the presence of bacteria (Fig. 7A). It would be interesting to investigate the molecular mechanisms involved in such overexpression of GT induced by *P. aeruginosa*. There was little influence of *phzA1* and *phzA2* mutations on the gliotoxin production in normoxia compared to wild type *P. aeruginosa*. However, lack of *phzA2* function upon hypoxia dramatically decreased gliotoxin production, which might correlate with higher levels

of phenazines, except for PYO, under this condition (Fig. 3). Furthermore, we showed that an *A. fumigatus* Δ*gliT* mutant, impaired in gliotoxin production, had less growth in the presence of *P. aeruginosa* in normoxia conditions, emphasizing its importance for controlling bacterial growth. Further work is needed to investigate if gliotoxin indeed has a direct role in the *A. fumigatus-P. aeruginosa* interaction and to unravel its effects in bacterial physiology in mixed biofilms.

*P. aeruginosa* produces iron chelators that may cause an iron starvation environment for the fungus that results in its anti-*Aspergillus* effect. However, the fungus counterattacks the iron deficiency by also producing siderophores (21). Siderophores are ferric iron chelators, structurally separated into different classes named hydroxamates, catecholates, carboxylates, phenolates, and mixed class. Hydroxamates are subdivided into rhodotorulic acid-, ferrioxamine-, fusarinine-, coprogen-, and ferrichrome-type siderophores and are the ones that are produced by *A. fumigatus* (54). In our assay, fusarinine B, coprogen B, and ferrichrome were detected in monoculture and cocultures. The RPMI medium was an iron-deficient medium, similar to human plasma, and that is probably the reason why *A. fumigatus* produced many siderophores in monoculture. However, only ferrichrome, ferricrocin, and triacetylfusigen were produced by *A. fumigatus* in the presence of *P. aeruginosa* during biofilm formation in both normoxia and hypoxia. Ferrichrome and ferricrocin were produced in comparable amounts in the presence of both *P. aeruginosa* wild-type and mutant strains upon normoxia or hypoxia. However, triacetylfusigen was produced in larger amounts in the presence of the *P. aeruginosa* wild type than the mutant strains. In hypoxia conditions, fusarinine B was produced only in the presence of the *P. aeruginosa* Δ*phzA2* mutant, again indicating an interaction between the *phz* operons and *A. fumigatus* SM production. Previously, the importance of *A. fumigatus* siderophores for the iron competition with *P. aeruginosa* has been reported, and the participation of several genetic determinants (*hapX*, *sidA*, *sidF*, *sidG*, and *mirB*) involved in iron starvation adaptation in response to *P. aeruginosa* 1-HP has been demonstrated (17, 44, 45, 55). However, to the best of our knowledge this is the first time *A. fumigatus* siderophores have been directly identified during *A. fumigatus-P. aeruginosa* coculture biofilm formation.

*A. fumigatus* also produced pyripyropene in monoculture or dual cultures. Pyripyropene A was originally identified as a potent inhibitor of acyl-CoA cholesterol acyltransferase (56–58), a mammalian intracellular enzyme located in the endoplasmic reticulum that forms cholesteryl esters from cholesterol (59). Pyripyropene A also shows insecticidal activity against agricultural insect pests (58, 60). It is not known if there is any correlation between these activities and aspergillosis or in the competition with bacteria, and its identification in *A. fumigatus- P. aeruginosa* dual cultures is a completely novel observation. In our mixed biofilm settings, the bacterial target remains to be uncovered.

Other SM secreted by the fungus during the coculture interaction belong to the superpathway of fumitremorgin; these SM are prenylated indole alkaloid compounds produced by *A. fumigatus* and *Penicillium* spp. that can act as mycotoxins (61). All the compounds identified in the fumitremorgin superpathway are produced during *A. fumigatus* biofilm formation. However, only demethoxyfumitremorgin C and fumitremorgin are produced during the interaction with *P. aeruginosa* wild-type and mutant strains. Curiously, brevianamide F is produced only upon hypoxia in the presence of *P. aeruginosa* wild type but not mutant strains, which suggests that *phzA1* and *phzA2* functions are important for brevianamide F production. Demethoxyfumitremorgin C has been shown to inhibit the cell viability and induce apoptosis of PC3 human advanced prostate cancer cells (62). Fumitremorgin C has been described as an inhibitor of a multidrug resistance protein that mediates resistance to chemotherapeutics in breast cancer treatment, inhibiting the growth of several phytopathogenic fungi, showing lethality to brine shrimp, and displaying antifeedant activity toward armyworm (63–65). We also observed fumiquinazolines, which normally accumulate in *A. fumigatus* conidia (66) and are secreted during both monoculture and dual cultures of *A. fumigatus* and *P. aeruginosa* in hypoxia. It has been reported that fumiquinazoline F from *Penicillium coryphilum* has antibacterial activity against *Staphylococcus aureus* and

*Micrococcus luteus* (67). It remains to be investigated if all these compounds can affect *P. aeruginosa* physiology and growth and their mechanisms of action, if any.

In conclusion, we have annotated several SM secreted during *A. fumigatus* and *P. aeruginosa* biofilm formation, and this has provided several opportunities to understand the interaction between these two species. Further work will concentrate on the investigation of the roles of selected compounds in both fungal and bacterial competitors, and future data may be used for the development of novel drugs for the management of chronic infections that affect cystic fibrosis patients or other immunocompromised individuals.

## MATERIALS AND METHODS

***P. aeruginosa* and *A. fumigatus* strains and growth conditions.** The following species and strains were used in this work: *P. aeruginosa* UCBPP-PA14 (wild type [68]), Δ*phzA1* (PA14 *phzA1::Mr7* [69]), and Δ*phzA2* (PA14 with an in-frame deletion in *phzA2*; a gift from E. Déziel), and *A. fumigatus* CEA17, Δ*gliT*, Δ*psoF*, Δ*fmqA*, and Δ*fapR*. *P. aeruginosa* was grown from frozen stocks ([LB] medium plus 20% glycerol) in solid LB for 24h at 37°C. A single colony was transferred to 30 mL of LB and cultured overnight at 37°C, 200 rpm. The culture was centrifuged at 4,000 × *g*, for 5 min, and the pellet was washed with 10 mL of phosphate-buffered saline (PBS). After centrifugation, the pellet was resuspended in LB and the inoculum was adjusted, using a spectrophotometer, to an optical density at 600 nm ($OD_{600}$) of 0.07 to 0.075. This inoculum was grown in 30 mL of LB at 37°C, 200 rpm, for 5 h, and the centrifugation and PBS washing processes were repeated. The final pellet was resuspended in RPMI-HEPES, and the inoculum was adjusted to an OD of 0.07 to 0.075 (approximately $5 \times 10^8$ to $8 \times 10^8$ CFU/mL).

*A. fumigatus* strains were grown from frozen stocks, and conidia suspensions were obtained by harvesting grown mycelia on minimal medium plates as described by Ries and colleagues (70).

**Dual biofilm formation between *P. aeruginosa* and *A. fumigatus*.** To measure the interaction between *P. aeruginosa* and *A. fumigatus* and to determine the SM produced by them in single or cocultures, $1 \times 10^5$ CFU/mL of *P. aeruginosa* were inoculated with or without $1 \times 10^6$ conidia/mL of *A. fumigatus* in 15 mL of RPMI-HEPES medium into polystyrene Petri dishes (60 × 15 mm) under hypoxic (1% $O_2$, 5% $CO_2$) or normoxic (approximately 20% $O_2$ and 0.04% $CO_2$) conditions, at 37°C. After 5 days, the supernatant was collected, the plate was washed with 10 mL of ultrapure water to collect the cells, and both were transferred to a 50-mL tube. This mixture was centrifuged at 4,000 × *g* for 15 min at 4°C to obtain the pellet, which was used for qPCR assays, and the supernatant (20 mL), which was filtered through a 0.22-μm filter, was frozen and lyophilized for SM extraction.

On the bottom of the small Petri dishes used in this experiment, biofilm production was measured by the crystal violet (CV) method. The biofilm was dried at 37°C for 30 min and then stained with 5 mL of 0.05% (wt/vol) CV for 10 min. The plates were washed with 50 mL of PBS, and the CV was solubilized with 3 mL of 95% ethanol. Samples of 100 μL were transferred to 96-well plates, and the absorbance at 595 nm was determined, as a measure for biofilm formation.

**Dual quantification of species-specific biofilm growth by qPCR.** For DNA extraction, pellets obtained from cultures for evaluating the *P. aeruginosa-A. fumigatus* interaction were frozen and lyophilized before being triturated by adding 2-mm glass beads and 0.1-mm zirconia-silica beads and vortexing for 5 min. To the resulting powder, 1 mL of extraction buffer was added, and the tubes were vortexed for 5 min. Tubes were incubated in a water bath at 70°C for 45 min; every 10 to 15 min, the tubes were removed from the water bath and vortexed for 5 min. One milliliter of phenol-chloroform (1:1) was added to the mixture, and tubes were vortexed for 5 min. The content was transferred to 2-mL tubes and centrifuged at 14,000 × *g* for 15 min at room temperature. The supernatants were collected and transferred to 1.5-mL tubes, and 600 μL of isopropanol (Merck) was added. Samples were incubated at 4°C for 1 h before being centrifuged at 14,000 × *g* for 15 min at 4°C. The supernatant was discarded, the pellet was washed with 200 μL of 70% ethanol, and air dried for 15 min at room temperature, after which the pellet was resuspended in deionized water and treated with RNase (Promega).

*P. aeruginosa* DNA was specifically quantified by qPCR with primers for *ecfX* (ecfX-F, 5′-CGCATGCCTATCAGG CGTT-3′, and ecfX-R, 5′-GAACTGCCCAGGTGCTTGC-3′) and *gyrB* (gyrB-F, 5′-CCTGACCATCCGTCGCCACAAC-3′, and gyrB-R, 5′-CGCAGCAGGATGCCGACGCC-3′) (29, 30). *A. fumigatus* was quantified by amplification of 18S rDNA (18S fw, 5′-GACCTCGGCCCTTAAATAGC-3′, and 18S rv, 5′-CTCGGCCAAGGTGATGTACT-3′). The 10-μL qPCR mixture was composed of 5 μL SYBR green PCR master mix (Applied Biosystems, Foster City, CA, USA), 2.5 pmol of each primer, and 100 ng DNA. Cycling was performed on the ABI 7500 fast real-time PCR system with an initial hold at 95°C for 15 min, followed by 45 cycles at 95°C for 15 s and 60°C for 1 min, with a cycle threshold of 35. Negative controls without DNA were included in each qPCR run.

**SM extraction and UHPLC-HRMS² analysis.** SM were extracted from 50 mg freeze-dried sample of the entire supernatant of each sample by resuspension in 1 mL of HPLC-grade methanol (MeOH), followed by 1 h of sonication in an ultrasonic bath. For sample preparation, 500 μL of each obtained extract was filtered (0.22-μm filter), transferred to vials, and diluted with HPLC-grade MeOH to a total volume of 1 mL.

UHPLC-HRMS² positive-mode analysis was performed in a Thermo Scientific QExactive hybrid Quadrupole-Orbitrap mass spectrometer coupled to a Dionex UltiMate 3000 RSLCnano UHPLC system. For the stationary phase, a Thermo Scientific column, Accucore $C_{18}$ 2.6 μm (2.1 mm by 100 mm) was used. The mobile phase was 0.1% formic acid (A) and acetonitrile plus 0.1% formic acid (B). Eluent profiles (A/B percentages) were 95/5 up to 2/98 within 10 min, maintaining 2/98 for 5 min, down to 95/5 within 1.2 min, and maintaining

for 8.8 min. Total run time was 20 min for each run, and flow rate was 0.3 mL · $min^{-1}$. The injection volume was 5 $\mu$L. MS spectra were acquired with *m/z* ranges from 100 to 1,500, with 70,000 for mass resolution. Ionization parameters were a sheath gas flow rate of 45 $L.h^{-1}$, auxiliary gas flow rate of 10 $L.h^{-1}$, sweep gas flow rate of 2 $L.h^{-1}$, spray voltage of 3.5 kV, capillary temperature of 250°C, S-lens RF level of 50, and auxiliary gas heater temperature of 400°C. $MS^2$ spectra were acquired in data-dependent acquisition mode. Normalized collision energy was applied stepwise (20, 30, and 40) V, and the 5 most intense precursors per cycle were measured with 17,500 resolution.

**UHPLC-HRMS² data processing and FBMN.** Raw UHPLC-$HRMS^2$ data were converted into mzXML format files using MSConvert (71), with 32-bit binary encoding precision, zlib compression, and peak peaking. Feature detection was performed in MZmine2 (v.2.53) (72). For $MS^1$ spectra mass detection, an intensity threshold of 1E5 was used, and for $MS^2$ an intensity threshold of 1E3 was used. For $MS^1$ chromatogram building (73), a 5-ppm mass accuracy and a minimum peak intensity of 5E5 was set. Extracted ion chromatograms (XICs) were deconvolved using the baseline cut-off algorithm at an intensity of 1E5, minimum peak height of 3E5, and a peak duration range from 0.05 to 2 min. After chromatographic deconvolution, XICs were matched to $MS^2$ spectra within *m/z* 0.02 and 0.2-min retention time windows. Isotope peaks were grouped with 5-ppm mass tolerance, 0.1-min retention time tolerance, and a maximum charge of 2. Detected peaks in different samples were aligned with a 5-ppm tolerance, 75% weight for *m/z* determinations, and 25% for retention time. $MS^1$ features without $MS^2$ features assigned were filtered out of the resulting matrix as well as features that did not contain isotope peaks and that did not occur in at least three samples. Finally, the feature table was exported as a .csv file, and corresponding $MS^2$ spectra were exported as .mgf files. Features observed in blank samples were filtered.

A molecular network was created with the feature-based molecular networking (FBMN) workflow (74) on GNPS (https://gnps.ucsd.edu) (75). The data were filtered by removing all $MS^2$ fragment ions within 17 Da of the precursor *m/z*. $MS^2$ spectra were window filtered by choosing only the top 6 fragment ions in the ±50-Da window throughout the spectrum. The precursor ion mass tolerance was set to 0.02 Da, and the $MS^2$ fragment ion tolerance was set to 0.02 Da. A molecular network was then created in which edges were filtered to have a cosine score above 0.65 and more than 4 matched peaks. Furthermore, edges between two nodes were kept in the network if and only if each of the nodes appeared in each other's respective top 10 most similar nodes. Finally, the maximum size of a molecular family was set to 100, and the lowest-scoring edges were removed from molecular families until the molecular family size was below this threshold. The spectra in the network were then searched against GNPS spectral libraries (75, 76). The library spectra were filtered in the same manner as the input data. All matches kept between network spectra and library spectra were required to have a score above 0.65 and at least 4 matched peaks. Dereplicator Plus was used to annotate MS/MS spectra (77). The molecular networks were visualized using Cytoscape software (78). Resulting networks were displayed and analyzed with Cytoscape (v.3.8.2).

**Metabolite annotation.** For SM dereplication, metabolites were annotated based on the GNPS $MS^2$ database via the FBMN and Dereplicator Plus workflows available on the GNPS platform. Other metabolites were manually searched against natural products databases such as the Dictionary of Natural Products, and the acquired $MS^2$ spectra were compared to spectra deposited either on the GNPS database or previously published in the literature. The compounds gliotoxin, gliotoxin E, pseurotin E, and spirotryprostatin A were annotated based on their exact masses.

**Data availability.** The molecular networking job can be publicly accessed at https://gnps.ucsd.edu/ProteoSAFe/status.jsp?task=0b027bfab9064518945341d3c24ba2a9, and the Dereplicator Plus job can be accessed at https://gnps.ucsd.edu/ProteoSAFe/status.jsp?task=415264520a41492a9b43b47e623028ed for hypoxia conditions and at https://gnps.ucsd.edu/ProteoSAFe/status.jsp?task=08a9ebb5609745d5a6f805896e527b67 and https://gnps.ucsd.edu/ProteoSAFe/status.jsp?task=e59e11f719cf4ae5beb406090a987f01 for normoxia.

## ACKNOWLEDGMENTS

We thank Fundação de Amparo à Pesquisa do Estado de São Paulo (FAPESP) 2017/19821-5 (R.W.B.), 2017/07536-4 (A.C.C.), 2016/12948-7 (P.A.C.) 2016/07870-9 (G.H.G.), 2021/07038-0 (D.A.), 2021/00728-0 (T.F.), and 2021/11062-3 (R.L.B.), and Conselho Nacional de Desenvolvimento Científico e Tecnológico (CNPq) 301058/2019-9 and 404735/2018-5 (G.H.G.), both from Brazil, and also a National Institutes of Health National Institute of Allergy and Infectious Diseases grant (R01AI153356) from the United States. This study was financed in part by the Coordenação de Aperfeiçoamento de Pessoal de Nível Superior—Brasil (CAPES)—Finance Code 001 (R.S.L.). We also thank the two anonymous reviewers for their comments and suggestions.

## REFERENCES

1. Beswick E, Amich J, Gago S. 2020. Factoring in the complexity of the cystic fibrosis lung to understand *Aspergillus fumigatus* and *Pseudomonas aeruginosa* interactions. Pathogens 9:639. https://doi.org/10.3390/pathogens9080639.
2. Vilaplana L, Marco MP. 2020. Phenazines as potential biomarkers of *Pseudomonas aeruginosa* infections: synthesis regulation, pathogenesis and analytical methods for their detection. Anal Bioanal Chem 412:5897–5912. https://doi.org/10.1007/s00216-020-02696-4.
3. Haq IJ, Gardner A, Brodlie M. 2016. A multifunctional bispecific antibody against *Pseudomonas aeruginosa* as a potential therapeutic strategy. Ann Transl Med 4:12. https://doi.org/10.3978/j.issn.2305-5839.2015.10.10.
4. Worlitzsch D, Tarran R, Ulrich M, Schwab U, Cekici A, Meyer KC, Birrer P, Bellon G, Berger J, Weiss T, Botzenhart K, Yankaskas JR, Randell S, Boucher RC, Döring G. 2002. Effects of reduced mucus oxygen concentration in airway

*Pseudomonas* infections of cystic fibrosis patients. J Clin Invest 109:317–325. https://doi.org/10.1172/JCI13870.
5. Olivares E, Badel-Berchoux S, Provot C, Prévost G, Bernardi T, Jehl F. 2019. Clinical impact of antibiotics for the treatment of *Pseudomonas aeruginosa* biofilm infections. Front Microbiol 10:2894. https://doi.org/10.3389/fmicb.2019.02894.
6. Bastos RW, Rossato L, Goldman GH, Santos DA. 2021. Fungicide effects on human fungal pathogens: cross-resistance to medical drugs and beyond. PLoS Pathog 17:e1010073. https://doi.org/10.1371/journal.ppat.1010073.
7. Burks C, Darby A, Gómez Londoño L, Momany M, Brewer MT. 2021. Azole-resistant *Aspergillus fumigatus* in the environment: identifying key reservoirs and hotspots of antifungal resistance. PLoS Pathog 17:e1009711. https://doi.org/10.1371/journal.ppat.1009711.
8. Latgé JP, Chamilos G. 2019. *Aspergillus fumigatus* and aspergillosis in 2019. Clin Microbiol Rev 33:e00140-18. https://doi.org/10.1128/CMR.00140-18.
9. Baxter CG, Dunn G, Jones AM, Webb K, Gore R, Richardson MD, Denning DW. 2013. Novel immunologic classification of aspergillosis in adult cystic fibrosis. J Allergy Clin Immunol 132:560–566.e10. https://doi.org/10.1016/j.jaci.2013.04.007.
10. Moss A, Juarez-Colunga E, Nathoo F, Wagner B, Sagel S. 2016. A comparison of change point models with application to longitudinal lung function measurements in children with cystic fibrosis. Stat Med 35:2058–2073. https://doi.org/10.1002/sim.6845.
11. Agarwal R, Sehgal IS, Dhooria S, Aggarwal AN. 2016. Developments in the diagnosis and treatment of allergic bronchopulmonary aspergillosis. Expert Rev Respir Med 10:1317–1334. https://doi.org/10.1080/17476348.2016.1249853.
12. Brandt C, Roehmel J, Rickerts V, Melichar V, Niemann N, Schwarz C. 2018. *Aspergillus* bronchitis in patients with cystic fibrosis. Mycopathologia 183:61–69. https://doi.org/10.1007/s11046-017-0190-0.
13. Bakare N, Rickerts V, Bargon J, Just-Nübling G. 2003. Prevalence of *Aspergillus fumigatus* and other fungal species in the sputum of adult patients with cystic fibrosis. Mycoses 46:19–23. https://doi.org/10.1046/j.1439-0507.2003.00830.x.
14. Amin R, Dupuis A, Aaron SD, Ratjen F. 2010. The effect of chronic infection with *Aspergillus fumigatus* on lung function and hospitalization in patients with cystic fibrosis. Chest 137:171–176. https://doi.org/10.1378/chest.09-1103.
15. Paugam A, Baixench M-T, Demazes-Dufeu N, Burgel P-R, Sauter E, Kanaan R, Dusser D, Dupouy-Camet J, Hubert D. 2010. Characteristics and consequences of airway colonisation by filamentous fungi in 201 adult patients with cystic fibrosis in France. Med Mycol 48:S32–S36. https://doi.org/10.3109/13693786.2010.503665.
16. Hector A, Kirn T, Ralhan A, Graepler-Mainka U, Berenbrinker S, Riethmueller J, Hogardt M, Wagner M, Pfleger A, Autenrieth I, Kappler M, Griese M, Eber E, Martus P, Hartl D. 2016. Microbial colonization and lung function in adolescents with cystic fibrosis. J Cyst Fibros 15:340–349. https://doi.org/10.1016/j.jcf.2016.01.004.
17. Briard B, Mislin GLA, Latgé JP, Beauvais A. 2019. Interactions between *Aspergillus fumigatus* and pulmonary bacteria: current state of the field, new data, and future perspective. J Fungi 5:48. https://doi.org/10.3390/jof5020048.
18. Briard B, Rasoldier V, Bomme P, ElAouad N, Guerreiro C, Chassagne P, Muszkieta L, Latgé J-P, Mulard L, Beauvais A. 2017. Dirhamnolipids secreted from *Pseudomonas aeruginosa* modify anjpegungal susceptibility of *Aspergillus fumigatus* by inhibiting beta1,3 glucan synthase activity. ISME J 11:1578–1591. https://doi.org/10.1038/ismej.2017.32.
19. Mowat E, Rajendran R, Williams C, McCulloch E, Jones B, Lang S, Ramage G. 2010. *Pseudomonas aeruginosa* and their small diffusible extracellular molecules inhibit *Aspergillus fumigatus* biofilm formation. FEMS Microbiol Lett 313:96–102. https://doi.org/10.1111/j.1574-6968.2010.02130.x.
20. Sass G, Nazik H, Penner J, Shah H, Ansari SR, Clemons KV, Groleau M-C, Dietl A-M, Visca P, Haas H, Deziel E, Stevens DA. 2018. Studies of *Pseudomonas aeruginosa* mutants indicate pyoverdine as the central factor in inhibition of *Aspergillus fumigatus* biofilm. J Bacteriol 200:e00345-17. https://doi.org/10.1128/JB.00345-17.
21. Sass G, Ansari SR, Dietl A-M, Déziel E, Haas H, Stevens DA. 2019. Intermicrobial interaction: *Aspergillus fumigatus* siderophores protect against competition by *Pseudomonas aeruginosa*. PLoS One 14:e0216085. https://doi.org/10.1371/journal.pone.0216085.
22. Zheng H, Kim J, Liew M, Yan JK, Herrera O, Bok JW, Kelleher NL, Keller NP, Wang Y. 2015. Redox metabolites signal polymicrobial biofilm development via the NapA oxidative stress cascade in *Aspergillus*. Curr Biol 25:29–37. https://doi.org/10.1016/j.cub.2014.11.018.
23. Kerr JR, Taylor GW, Rutman A, Hoiby N, Cole PJ, Wilson R. 1999. *Pseudomonas aeruginosa* pyocyanin and 1-hydroxyphenazine inhibit fungal growth. J Clin Pathol 52:385–387. https://doi.org/10.1136/jcp.52.5.385.
24. Nishanth Kumar S, Nisha GV, Sudaresan A, Venugopal VV, Sree Kumar MM, Lankalapalli RS, Dileep Kumar BS. 2014. Synergistic activity of phenazines isolated from *Pseudomonas aeruginosa* in combination with azoles against Candida species. Med Mycol 52:482–490. https://doi.org/10.1093/mmy/myu012.
25. Sass G, Nazik H, Chatterjee P, Stevens DA. 2021. Under nonlimiting iron conditions pyocyanin is a major antifungal molecule, and differences between prototypic *Pseudomonas aeruginosa* strains. Med Mycol 59:453–464. https://doi.org/10.1093/mmy/myaa066.
26. Ramos AN, Peral MC, Valdez JC. 2010. Differences between *Pseudomonas aeruginosa* in a clinical sample and in a colony isolated from it: comparison of virulence capacity and susceptibility of biofilm to inhibitors. Comp Immunol Microbiol Infect Dis 33:267–275. https://doi.org/10.1016/j.cimid.2008.10.004.
27. Du X, Li Y, Zhou Q, Xu Y. 2015. Regulation of gene expression in *Pseudomonas aeruginosa* M18 by phenazine-1-carboxylic acid. Appl Microbiol Biotechnol 99:813–825. https://doi.org/10.1007/s00253-014-6101-0.
28. Lau GW, Hassett DJ, Ran H, Kong F. 2004. The role of pyocyanin in *Pseudomonas aeruginosa* infection. Trends Mol Med 10:599–606. https://doi.org/10.1016/j.molmed.2004.10.002.
29. Qin X, Emerson J, Stapp J, Stapp L, Abe P, Burns JL. 2003. Use of realtime PCR with multiple targets to identify Pseudomonas aeruginosa and other nonfermenting gram-negative bacilli from patients with cystic fibrosis. J Clin Microbiol 41:4312–4317. https://doi.org/10.1128/JCM.41.9.4312-4317.2003.
30. Lavenir R, Jocktane D, Laurent F, Nazaret S, Cournoyer B. 2007. Improved reliability of *Pseudomonas aeruginosa* PCR detection by the use of the species-specific *ecfX* gene target. J Microbiol Methods 70:20–29. https://doi.org/10.1016/j.mimet.2007.03.008.
31. Anuj SN, Whiley DM, Kidd TJ, Bell SC, Wainwright CE, Nissen MD, Sloots TP. 2009. Identification of *Pseudomonas aeruginosa* by a duplex real-time polymerase chain reaction assay targeting the *ecfX* and the *gyrB* genes. Diagn Microbiol Infect Dis 63:127–131. https://doi.org/10.1016/j.diagmicrobio.2008.09.018.
32. Barakat R, Goubet I, Manon S, Berges T, Rosenfeld E. 2014. Unsuspected pyocyanin effect in yeast under anaerobiosis. Microbiologyopen 3:1–14. https://doi.org/10.1002/mbo3.142.
33. Steffan N, Grundmann A, Yin WB, Kremer A, Li SM. 2009. Indole prenyltransferases from fungi: a new enzyme group with high potential for the production of prenylated indole derivatives. Curr Med Chem 16:218–231. https://doi.org/10.2174/092986709787002772.
34. Girardin H, Latge JP, Srikantha T, Morrow B, Soll DR. 1993. Development of DNA probes for fingerprinting Aspergillus fumigatus. J Clin Microbiol 31:1547–1554. https://doi.org/10.1128/jcm.31.6.1547-1554.1993.
35. Monod M, Paris S, Sarfati J, Jaton-Ogay K, Ave P, Latge JP. 1993. Virulence of alkaline protease-deficient mutants of Aspergillus fumigatus. FEMS Microbiol Lett 106:39–46. https://doi.org/10.1111/j.1574-6968.1993.tb05932.x.
36. Bertuzzi M, van Rhijn N, Krappmann S, Bowyer P, Bromley MJ, Bignell EM. 2021. On the lineage of Aspergillus fumigatus isolates in common laboratory use. Med Mycol 59:7–13. https://doi.org/10.1093/mmy/myaa075.
37. Wiehlmann L, Wagner G, Cramer N, Siebert B, Gudowius P, Morales G, Köhler T, van Delden C, Weinel C, Slickers P, Tümmler B. 2007. Population structure of *Pseudomonas aeruginosa*. Proc Natl Acad Sci U S A 104:8101–8106. https://doi.org/10.1073/pnas.0609213104.
38. Yadav V, Gupta J, Mandhan R, Chhillar AK, Dabur R, Singh DD, Sharma GL. 2005. Investigations on anti-Aspergillus properties of bacterial products. Lett Appl Microbiol 41:309–314. https://doi.org/10.1111/j.1472-765X.2005.01772.x.
39. Anand R, Clemons KV, Stevens DA. 2017. Effect of anaerobiasis or hypoxia on *Pseudomonas aeruginosa* inhibition of *Aspergillus fumigatus* biofilm. Arch Microbiol 199:881–890. https://doi.org/10.1007/s00203-017-1362-5.
40. Price-Whelan A, Dietrich LE, Newman DK. 2007. Pyocyanin alters redox homeostasis and carbon flux through central metabolic pathways in *Pseudomonas aeruginosa* PA14. J Bacteriol 189:6372–6381. https://doi.org/10.1128/JB.00505-07.
41. Reece E, Doyle S, Greally P, Renwick J, McClean S. 2018. *Aspergillus fumigatus* inhibits *Pseudomonas aeruginosa* in co-culture: implications of a mutually antagonistic relationship on virulence and inflammation in the CF airway. Front Microbiol 9:1205. https://doi.org/10.3389/fmicb.2018.01205.
42. Margalit A, Carolan JC, Sheehan D, Kavanagh K. 2020. The *Aspergillus fumigatus* secretome alters the proteome of *Pseudomonas aeruginosa* to stimulate bacterial growth: implications for co-infection. Mol Cell Proteomics 19:1346–1359. https://doi.org/10.1074/mcp.RA120.002059.
43. Filiatrault MJ, Picardo KF, Ngai H, Passador L, Iglewski BH. 2006. Identification of *Pseudomonas aeruginosa* genes involved in virulence and anaerobic growth. Infect Immun 74:4237–4245. https://doi.org/10.1128/IAI.02014-05.
44. Moree WJ, Phelan VV, Wu CH, Bandeira N, Cornett DS, Duggan BM, Dorrestein PC. 2012. Interkingdom metabolic transformations captured by microbial imaging mass spectrometry. Proc Natl Acad Sci U S A 109:13811–13816. https://doi.org/10.1073/pnas.1206855109.
45. Briard B, Bomme P, Lechner BE, Mislin GLA, Lair V, Prévost M-C, Latgé J-P, Haas H, Beauvais A. 2015. *Pseudomonas aeruginosa* manipulates redox

and iron homeostasis of its microbiota partner *Aspergillus fumigatus* via phenazines. Sci Rep 5:8220. https://doi.org/10.1038/srep08220.
46. Sultan M, Arya R, Kim KK. 2021. Roles of two-component systems in *Pseudomonas aeruginosa* virulence. Int J Mol Sci 22:12152. https://doi.org/10.3390/ijms222212152.
47. Recinos DA, Sekedat MD, Hernandez A, Cohen TS, Sakhtah H, Prince AS, Price-Whelan A, Dietrich LE. 2012. Redundant phenazine operons in *Pseudomonas aeruginosa* exhibit environment-dependent expression and differential roles in pathogenicity. Proc Natl Acad Sci U S A 109:19420–19425. https://doi.org/10.1073/pnas.1213901109.
48. Cui Q, Lv H, Qi Z, Jiang B, Xiao B, Liu L, Ge Y, Hu X. 2016. Cross-regulation between the phz1 and phz2 operons maintain a balanced level of phenazine biosynthesis in *Pseudomonas aeruginosa* PAO1. PLoS One 11: e0144447. https://doi.org/10.1371/journal.pone.0144447.
49. Schmitz S, Rosenbaum MA. 2020. Controlling the production of *Pseudomonas* phenazines by modulating the genetic repertoire. ACS Chem Biol 15:3244–3252. https://doi.org/10.1021/acschembio.0c00805.
50. Soberón-Chávez G, Lépine F, Déziel E. 2005. Production of rhamnolipids by *Pseudomonas aeruginosa*. Appl Microbiol Biotechnol 68:718–725. https://doi.org/10.1007/s00253-005-0150-3.
51. Margalit A, Sheehan D, Carolan JC, Kavanagh K. 2022. Exposure to the *Pseudomonas aeruginosa* secretome alters the proteome and secondary metabolite production of *Aspergillus fumigatus*. Microbiology (Reading) 168 https://doi.org/10.1099/mic.0.001164.
52. Bruns S, Seidler M, Albrecht D, Salvenmoser S, Remme N, Hertweck C, Brakhage AA, Kniemeyer O, Müller FM. 2010. Functional genomic profiling of *Aspergillus fumigatus* biofilm reveals enhanced production of the mycotoxin gliotoxin. Proteomics 10:3097–3107. https://doi.org/10.1002/pmic.201000129.
53. Dolan SK, O'Keeffe G, Jones GW, Doyle S. 2015. Resistance is not futile: gliotoxin biosynthesis, functionality and utility. Trends Microbiol 23: 419–428. https://doi.org/10.1016/j.tim.2015.02.005.
54. Aguiar M, Orasch T, Misslinger M, Dietl AM, Gsaller F, Haas H. 2021. The siderophore transporters Sit1 and Sit2 are essential for utilization of ferrichrome-, ferrioxamine- and coprogen-type siderophores in *Aspergillus fumigatus*. J Fungi 7:768. https://doi.org/10.3390/jof7090768.
55. Nazik H, Sass G, Ansari SR, Ertekin R, Haas H, Déziel E, Stevens DA. 2020. Novel intermicrobial molecular interaction: *Pseudomonas aeruginosa* quinolone signal (PQS) modulates *Aspergillus fumigatus* response to iron. Microbiology (Reading) 166:44–55. https://doi.org/10.1099/mic.0.000858.
56. Omura S, Tomoda H, Kim YK, Nishida H. 1993. Pyripyropenes, highly potent inhibitors of acyl-CoA:cholesterol acyltransferase produced by *Aspergillus fumigatus*. J Antibiot (Tokyo) 46:1168–1169. https://doi.org/10.7164/antibiotics.46.1168.
57. Tomoda H, Kim YK, Nishida H, Masuma R, Omura S. 1994. Pyripyropenes, novel inhibitors of acyl-CoA:cholesterol acyltransferase produced by *Aspergillus fumigatus*. I. Production, isolation, and biological properties. J Antibiot (Tokyo) 47:148–153. https://doi.org/10.7164/antibiotics.47.148.
58. Raffa N, Keller NP. 2019. A call to arms: mustering secondary metabolites for success and survival of an opportunistic pathogen. PLoS Pathog 15: e1007606. https://doi.org/10.1371/journal.ppat.1007606.
59. Spector AA, Mathur SN, Kaduce TL. 1979. Role of acylcoenzyme A: cholesterol o-acyltransferase in cholesterol metabolism. Prog Lipid Res 18: 31–53. https://doi.org/10.1016/0163-7827(79)90003-1.
60. Goto K, Horikoshi R, Nakamura S, Mitomi M, Oyama K, Hirose T, Sunazuka T, Ōmura S. 2019. Synthesis of pyripyropene derivatives and their pest-control efficacy. J Pestic Sci 44:255–263. https://doi.org/10.1584/jpestics.D19-032.
61. Maiya S, Grundmann A, Li SM, Turner G. 2006. The fumitremorgin gene cluster of *Aspergillus fumigatus*: identification of a gene encoding brevianamide F synthetase. Chembiochem 7:1062–1069. https://doi.org/10.1002/cbic.200600003.
62. Kim YS, Kim SK, Park SJ. 2017. Apoptotic effect of demethoxyfumitremorgin C from marine fungus *Aspergillus fumigatus* on PC3 human prostate cancer cells. Chem Biol Interact 269:18–24. https://doi.org/10.1016/j.cbi.2017.03.015.
63. Rabindran SK, Ross DD, Doyle LA, Yang W, Greenberger LM. 2000. Fumitremorgin C reverses multidrug resistance in cells transfected with the breast cancer resistance protein. Cancer Res 60:47–50.
64. González-Lobato L, Real R, Prieto JG, Alvarez AI, Merino G. 2010. Differential inhibition of murine Bcrp1/Abcg2 and human BCRP/ABCG2 by the mycotoxin fumitremorgin C. Eur J Pharmacol 644:41–48. https://doi.org/10.1016/j.ejphar.2010.07.016.
65. Li XJ, Zhang Q, Zhang AL, Gao JM. 2012. Metabolites from *Aspergillus fumigatus*, an endophytic fungus associated with *Melia azedarach*, and their antifungal, antifeedant, and toxic activities. J Agric Food Chem 60: 3424–3431. https://doi.org/10.1021/jf300146n.
66. Lim FY, Ames B, Walsh CT, Keller NP. 2014. Co-ordination between BrlA regulation and secretion of the oxidoreductase FmqD directs selective accumulation of fumiquinazoline C to conidial tissues in *Aspergillus fumigatus*. Cell Microbiol 16:1267–1283. https://doi.org/10.1111/cmi.12284.
67. Silva MG, Furtado NA, Pupo MT, Fonseca MJ, Said S, da Silva Filho AA, Bastos JK. 2004. Antibacterial activity from *Penicillium corylophilum* Dierckx. Microbiol Res 159:317–322. https://doi.org/10.1016/j.micres.2004.06.003.
68. Rahme LG, Stevens EJ, Wolfort SF, Shao J, Tompkins RG, Ausubel FM. 1995. Common virulence factors for bacterial pathogenicity in plants and animals. Science 268:1899–1902. https://doi.org/10.1126/science.7604262.
69. Liberati NT, Urbach JM, Miyata S, Lee DG, Drenkard E, Wu G, Villanueva J, Wei T, Ausubel FM. 2006. An ordered, nonredundant library of *Pseudomonas aeruginosa* strain PA14 transposon insertion mutants. Proc Natl Acad Sci U S A 103:2833–2838. https://doi.org/10.1073/pnas.0511100103.
70. Ries LNA, Beattie SR, Espeso EA, Cramer RA, Goldman GH. 2016. Diverse regulation of the CreA carbon catabolite repressor in *Aspergillus nidulans*. Genetics 203:335–352. https://doi.org/10.1534/genetics.116.187872.
71. Chambers MC, Maclean B, Burke R, Amodei D, Ruderman DL, Neumann S, Gatto L, Fischer B, Pratt B, Egertson J, Hoff K, Kessner D, Tasman N, Shulman N, Frewen B, Baker TA, Brusniak M-Y, Paulse C, Creasy D, Flashner L, Kani K, Moulding C, Seymour SL, Nuwaysir LM, Lefebvre B, Kuhlmann F, Roark J, Rainer P, Detlev S, Hemenway T, Huhmer A, Langridge J, Connolly B, Chadick T, Holly K, Eckels J, Deutsch EW, Moritz RL, Katz JE, Agus DB, MacCoss M, Tabb DL, Mallick P. 2012. A cross-platform toolkit for mass spectrometry and proteomics. Nat Biotechnol 30:918–920. https://doi.org/10.1038/nbt.2377.
72. Pluskal T, Castillo S, Villar-Briones A, Orešič M. 2010. MZmine 2: modular framework for processing, visualizing, and analyzing mass spectrometry-based molecular profile data. BMC Bioinformatics 11:395. https://doi.org/10.1186/1471-2105-11-395.
73. Myers OD, Sumner SJ, Li S, Barnes S, Du X. 2017. One step forward for reducing false positive and false negative compound identifications from mass spectrometry metabolomics data: new algorithms for constructing extracted ion chromatograms and detecting chromatographic peaks. Anal Chem 89: 8696–8703. https://doi.org/10.1021/acs.analchem.7b00947.
74. Nothias L-F, Petras D, Schmid R, Dührkop K, Rainer J, Sarvepalli A, Protsyuk I, Ernst M, Tsugawa H, Fleischauer M, Aicheler F, Aksenov AA, Alka O, Allard P-M, Barsch A, Cachet X, Caraballo-Rodriguez AM, Da Silva RR, Dang T, Garg N, Gauglitz JM, Gurevich A, Isaac G, Jarmusch AK, Kameník Z, Kang KB, Kessler N, Koester I, Korf A, Le Gouellec A, Ludwig M, Martin H C, McCall L-I, McSayles J, Meyer SW, Mohimani H, Morsy M, Moyne O, Neumann S, Neuweger H, Nguyen NH, Nothias-Esposito M, Paolini J, Phelan VV, Pluskal T, Quinn RA, Rogers S, Shrestha B, Tripathi A, van der Hooft JJJ, et al. 2020. Feature-based molecular networking in the GNPS analysis environment. Nat Methods 17:905–908. https://doi.org/10.1038/s41592-020-0933-6.
75. Wang M, Carver JJ, Phelan VV, Sanchez LM, Garg N, Peng Y, Nguyen DD, Watrous J, Kapono CA, Luzzatto-Knaan T, Porto C, Bouslimani A, Melnik AV, Meehan MJ, Liu W-T, Crüsemann M, Boudreau PD, Esquenazi E, Sandoval-Calderón M, Kersten RD, Pace LA, Quinn RA, Duncan KR, Hsu C-C, Floros DJ, Gavilan RG, Kleigrewe K, Northen T, Dutton RJ, Parrot D, Carlson EE, Aigle B, Michelsen CF, Jelsbak L, Sohlenkamp C, Pevzner P, Edlund A, McLean J, Piel J, Murphy BT, Gerwick L, Liaw C-C, Yang Y-L, Humpf H-U, Maansson M, Keyzers RA, Sims AC, Johnson AR, Sidebottom AM, Sedio BE, et al. 2016. Sharing and community curation of mass spectrometry data with Global Natural Products Social Molecular Networking. Nat Biotechnol 34:828–837. https://doi.org/10.1038/nbt.3597.
76. Horai H, Arita M, Kanaya S, Nihei Y, Ikeda T, Suwa K, Ojima Y, Tanaka K, Tanaka S, Aoshima K, Oda Y, Kakazu Y, Kusano M, Tohge T, Matsuda F, Sawada Y, Hirai MY, Nakanishi H, Ikeda K, Akimoto N, Maoka T, Takahashi H, Ara T, Sakurai N, Suzuki H, Shibata D, Neumann S, Iida T, Tanaka K, Funatsu K, Matsuura F, Soga T, Taguchi R, Saito K, Nishioka T. 2010. MassBank: a public repository for sharing mass spectral data for life sciences. J Mass Spectrom 45:703–714. https://doi.org/10.1002/jms.1777.
77. Mohimani H, Gurevich A, Shlemov A, Mikheenko A, Korobeynikov A, Cao L, Shcherbin E, Nothias L-F, Dorrestein PC, Pevzner PA. 2018. Dereplication of microbial metabolites through database search of mass spectra. Nat Commun 9:4035. https://doi.org/10.1038/s41467-018-06082-8.
78. Shannon P, Markiel A, Ozier O, Baliga NS, Wang JT, Ramage D, Amin N, Schwikowski B, Ideker T. 2003. Cytoscape: a software environment for integrated models of biomolecular interaction networks. Genome Res 13: 2498–2504. https://doi.org/10.1101/gr.1239303.